Recent developments in quantum magnetism

Gang Chen
Fudan University, Shanghai China

There is no field theory, no exotic phenomenon,
no fractionalization, no topological order, etc in this tutorial.

FUDAN UNIVERSITY 1905 复旦大学 FUDAN UNIVERSITY

Part 1 Topological magnons: the case of Weyl magnon

1. **What is Weyl semimetal?**
2. **Antiferromagnets and spin wave excitations**
3. **Weyl magnons: uniqueness and extension.**

Part 2 Detecting hidden multipolar orders in quantum magnets

1. **Hidden orders in condensed matter physics**
2. **Hidden orders with intertwined multipolar structure in rare-earth magnets**
3. **An experimental example**

復旦大學 FUDAN UNIVERSITY

Part 1 Topological magnons: the case of Weyl magnon

1. What is Weyl semimetal?

Selected for a Viewpoint in *Physics*

PHYSICAL REVIEW B **83**, 205101 (2011)

Topological semimetal and Fermi-arc surface states in the electronic structure of pyrochlore iridates

Xiangang Wan,[1] Ari M. Turner,[2] Ashvin Vishwanath,[2,3] and Sergey Y. Savrasov[1,4]

[1] *National Laboratory of Solid State Microstructures and Department of Physics, Nanjing University, Nanjing 210093, China*

[2] *Department of Physics, University of California, Berkeley, California 94720, USA*

[3] *Materials Sciences Division, Lawrence Berkeley National Laboratory, Berkeley, California 94720, USA*

[4] *Department of Physics, University of California, Davis, One Shields Avenue, Davis, California 95616, USA*

(Received 23 February 2011; published 2 May 2011)

Physics

Physics **4**, 36 (2011)

Viewpoint

Weyl electrons kiss

Leon Balents

Kavli Institute for Theoretical Physics, University of California, Santa Barbara, CA 93106, USA

Published May 2, 2011

Theorists predict the possibility of topological "Fermi arc" surface states in a system with broken time-reversal symmetry.

Subject Areas: **Strongly Correlated Materials**

Weyl semimetal

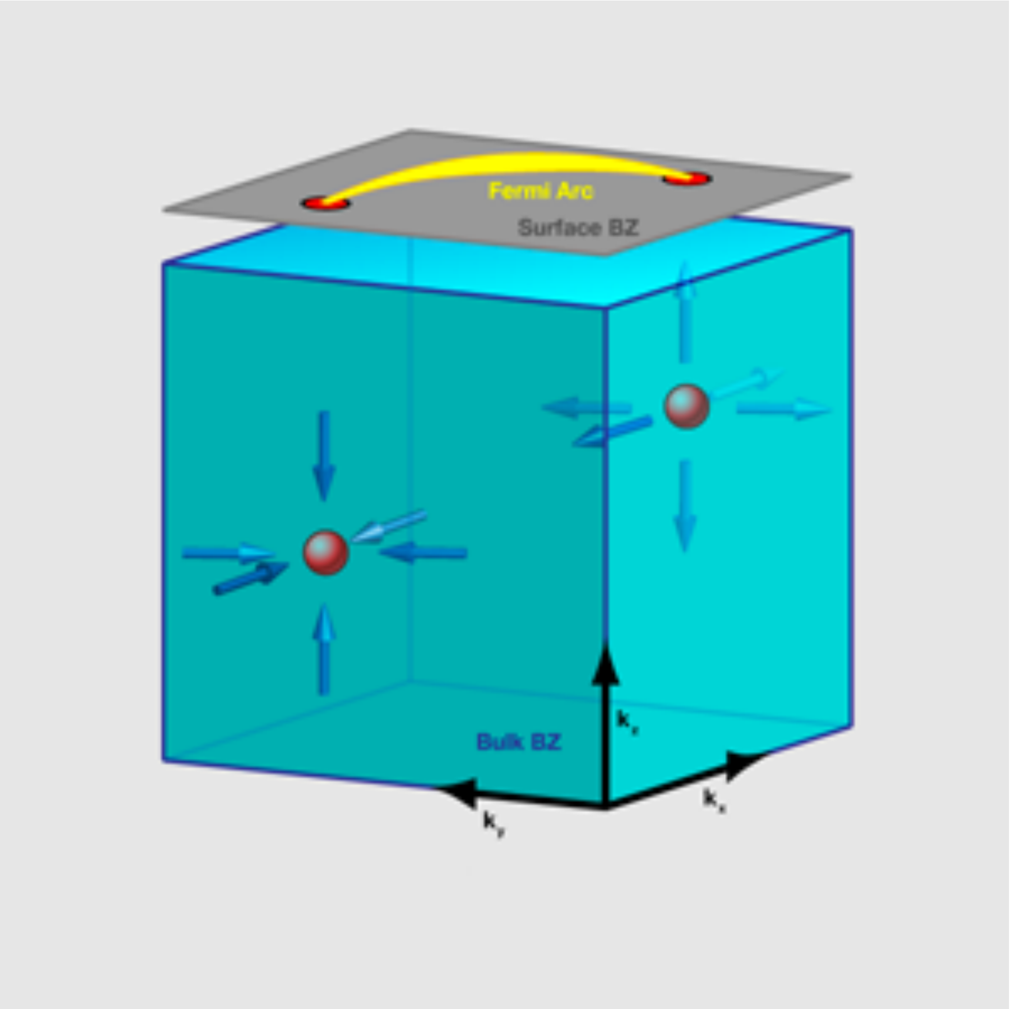

$$H_D = E_0 \mathbb{1} + \mathbf{v}_0 \cdot \mathbf{q} \mathbb{1} + \sum_{i=1}^{3} \mathbf{v}_i \cdot \mathbf{q} \sigma_i . \qquad (1)$$

Energy is measured from the chemical potential, $\mathbf{q} = \mathbf{k} - \mathbf{k}_0$

Weyl semimetal proposed in pyrochlore iridates

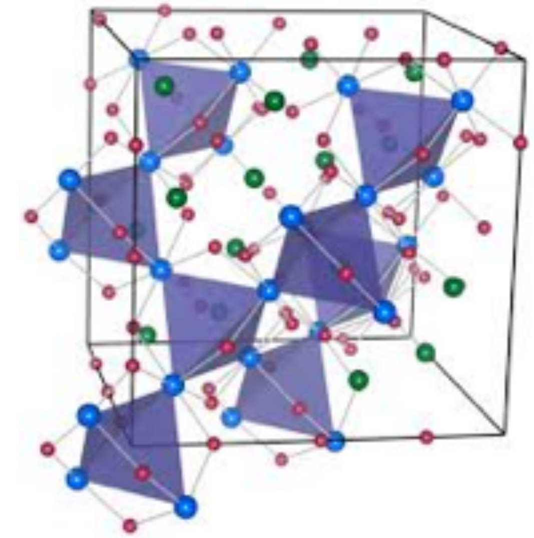

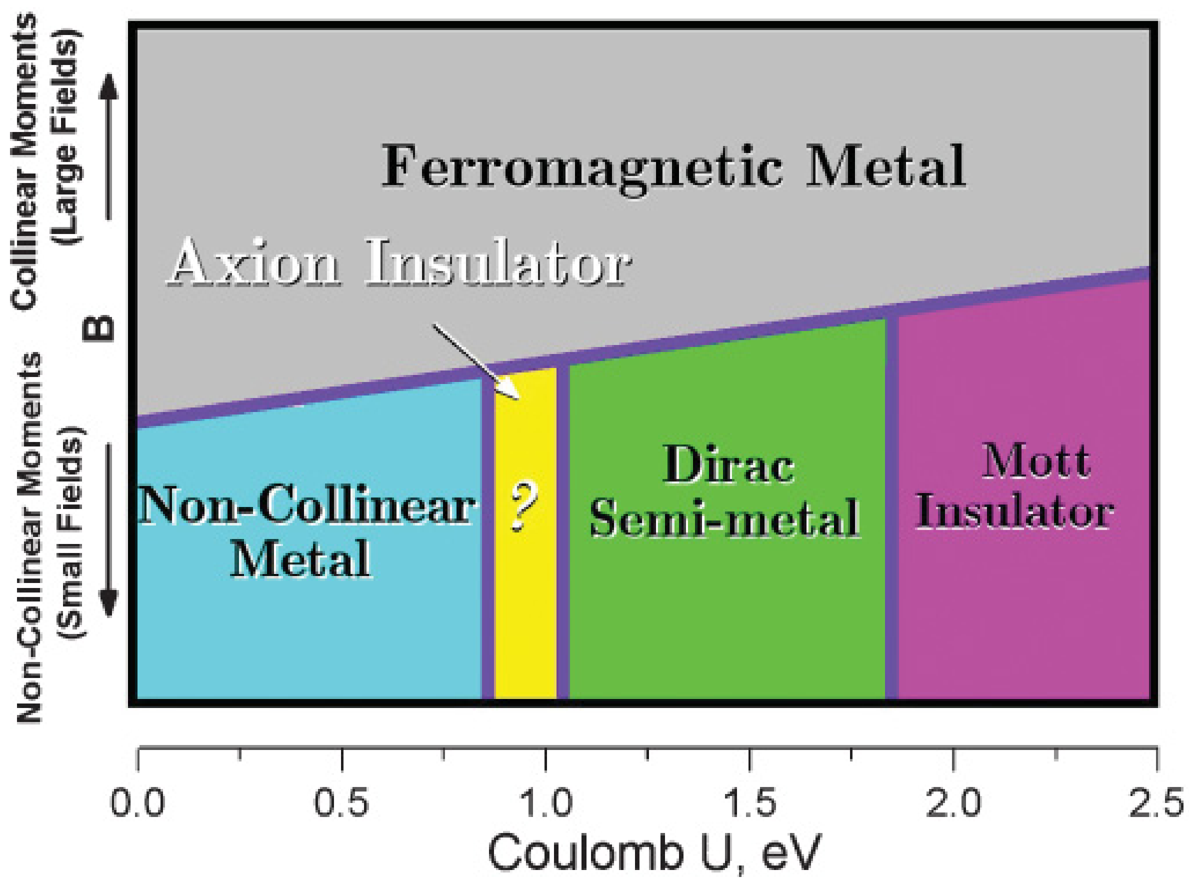

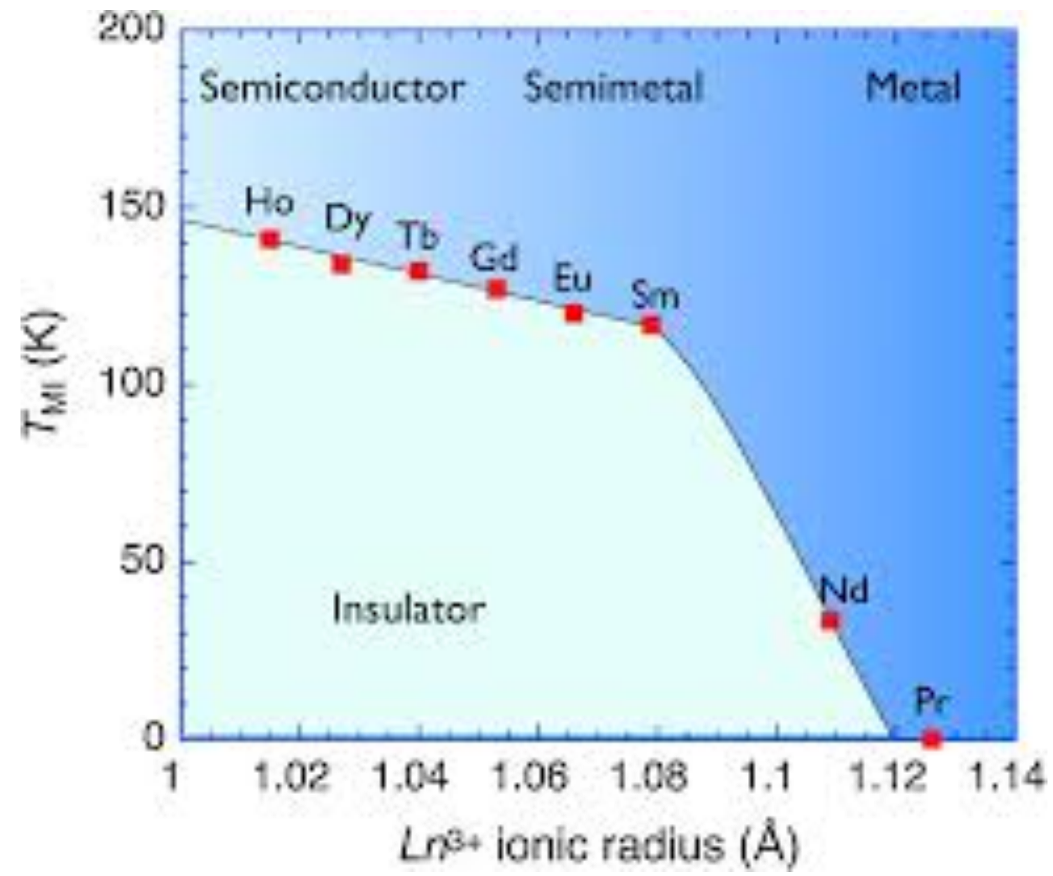

Xiangang Wan, Turner, Vishwanath, Savrasov, PhysRevB 2011,
Magnetic Weyl semimetal from the Ir correlation driven all-in all-out order.

复旦大学 FUDAN UNIVERSITY

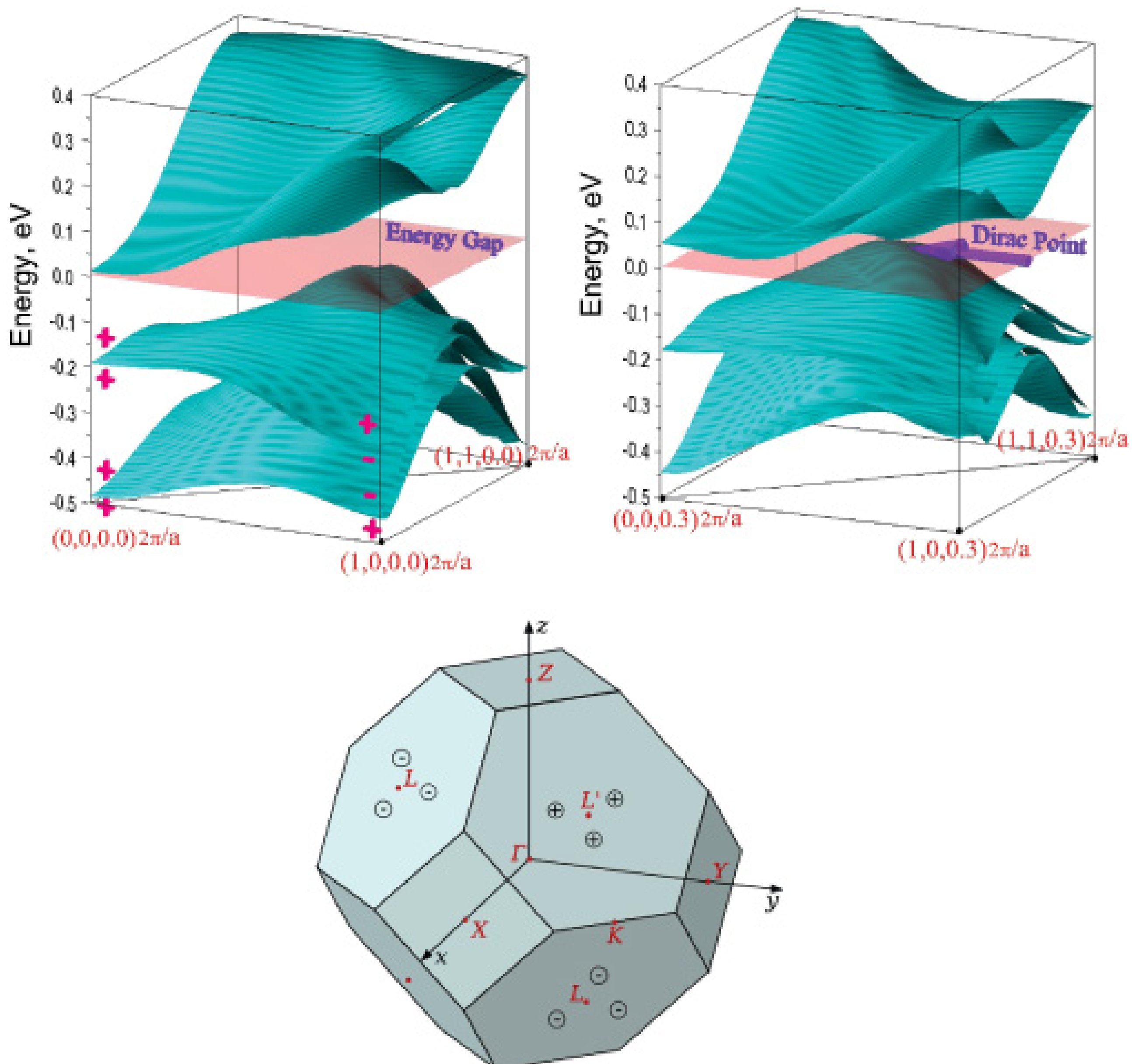

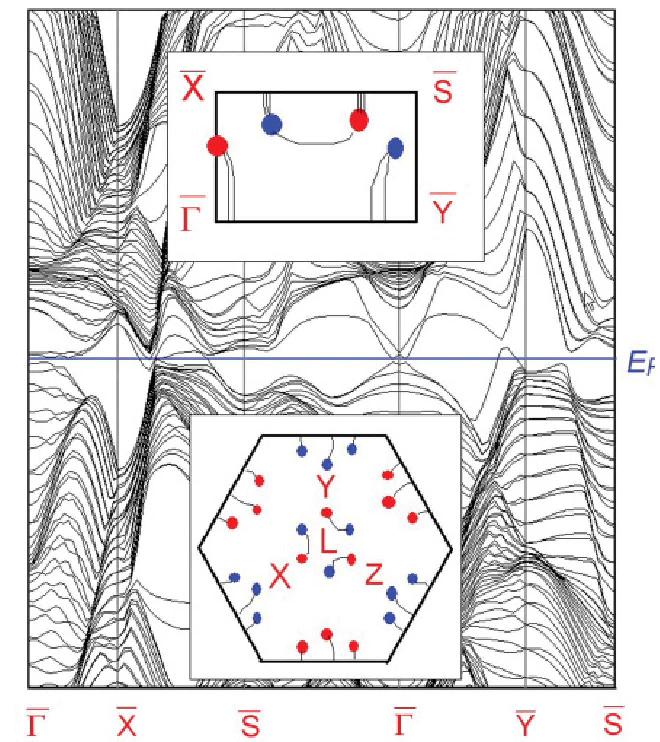

FIG. 4. (Color online) Semimetallic nature of the state at $U = 1.5$ eV according to the LSDA + U + SO method. (a) Calculated energy bands in the plane $K_z = 0$ with band parities shown; (b) energy bands in the plane $k_z = 0.6\pi/a$, where a Weyl point is predicted to exist. The lighter-shaded plane is at the Fermi level. (c) Locations of the Weyl points in the three-dimensional Brillouin zone (Ref. 29) (nine are shown, indicated by the circled + or − signs).

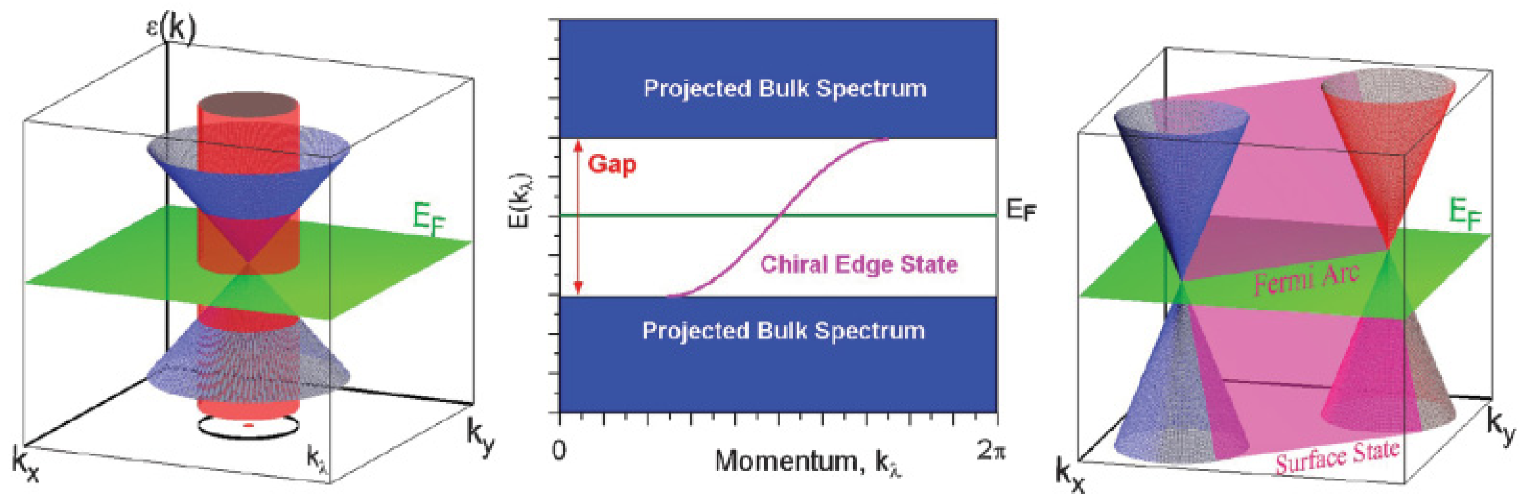

FIG. 5. (Color online) Illustration of surface states arising from bulk Weyl points. (a) The bulk states as a function of (k_x, k_y) (and arbitrary k_z) fill the inside of a cone. A cylinder whose base defines a one-dimensional circular Brillouin zone is also drawn. (b) The cylinder unrolled onto a plane gives the spectrum of the two-dimensional subsystem $H(\lambda, k_z)$ with a boundary. On top of the bulk spectrum, a chiral state appears due to the nonzero Chern number. (c) Meaning of the surface states back in the three-dimensional system. The chiral state appears as a surface connecting the original Dirac cone to a second one, and the intersection between this plane and the Fermi level gives a Fermi arc connecting the Weyl points.

The Weyl points behave like "magnetic" monopoles in momentum space whose charge is given by the chirality; they are actually a source of "Berry flux" rather than magnetic flux. The Berry connection, a vector potential in momentum space, is defined by $\mathcal{A}(\mathbf{k}) = \sum_{n=1}^{N} i\langle u_{n\mathbf{k}}|\nabla_{\mathbf{k}}|u_{n\mathbf{k}}\rangle$, where N is the number of occupied bands. As usual, the Berry flux is defined as $\mathcal{F} = \nabla_{\mathbf{k}} \times \mathcal{A}$. To show that there are arcs connecting pairs of Weyl points, we argue that there is an arc on the surface Brillouin zone emanating from the projection (k_{0x}, k_{0y}) of each Weyl point.

Weyl semimetal discovered in TaAs

TOPOLOGICAL MATTER

Discovery of a Weyl fermion semimetal and topological Fermi arcs

Su-Yang Xu,[1,2]* Ilya Belopolski,[1]* Nasser Alidoust,[1,2]* Madhab Neupane,[1,3]* Guang Bian,[1] Chenglong Zhang,[4] Raman Sankar,[5] Guoqing Chang,[6,7] Zhujun Yuan,[4] Chi-Cheng Lee,[6,7] Shin-Ming Huang,[6,7] Hao Zheng,[1] Jie Ma,[8] Daniel S. Sanchez,[1] BaoKai Wang,[6,7,9] Arun Bansil,[9] Fangcheng Chou,[5] Pavel P. Shibayev,[1,10] Hsin Lin,[6,7] Shuang Jia,[4,11] M. Zahid Hasan[1,2]†

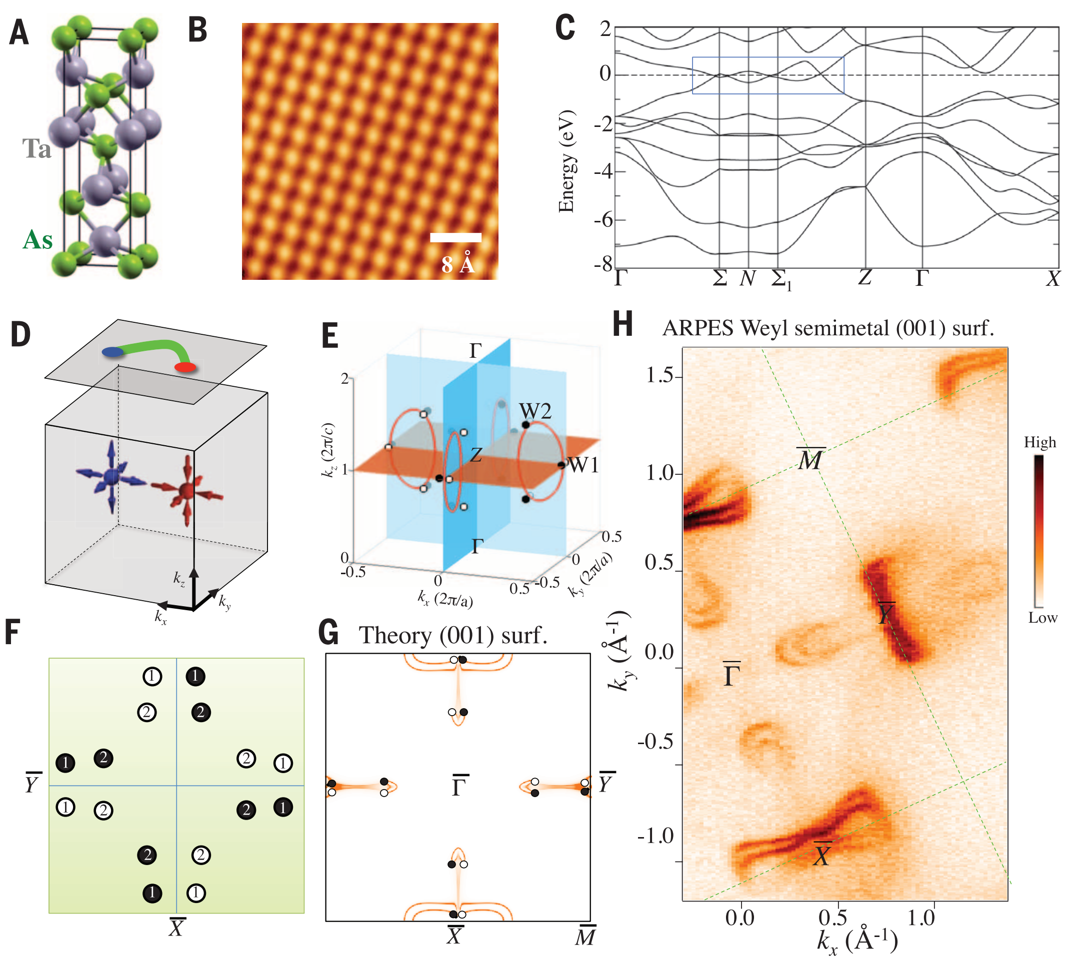

PHYSICAL REVIEW X 5, 031013 (2015)

Experimental Discovery of Weyl Semimetal TaAs

B. Q. Lv,[1] H. M. Weng,[1,2] B. B. Fu,[1] X. P. Wang,[2,3,1] H. Miao,[1] J. Ma,[1] P. Richard,[1,2] X. C. Huang,[1] L. X. Zhao,[1] G. F. Chen,[1,2] Z. Fang,[1,2] X. Dai,[1,2] T. Qian,[1,*] and H. Ding[1,2,†]
[1]Beijing National Laboratory for Condensed Matter Physics and Institute of Physics, Chinese Academy of Sciences, Beijing 100190, China
[2]Collaborative Innovation Center of Quantum Matter, Beijing, China
[3]Department of Physics, Tsinghua University, Beijing 100084, China
(Received 15 July 2015; published 31 July 2015)

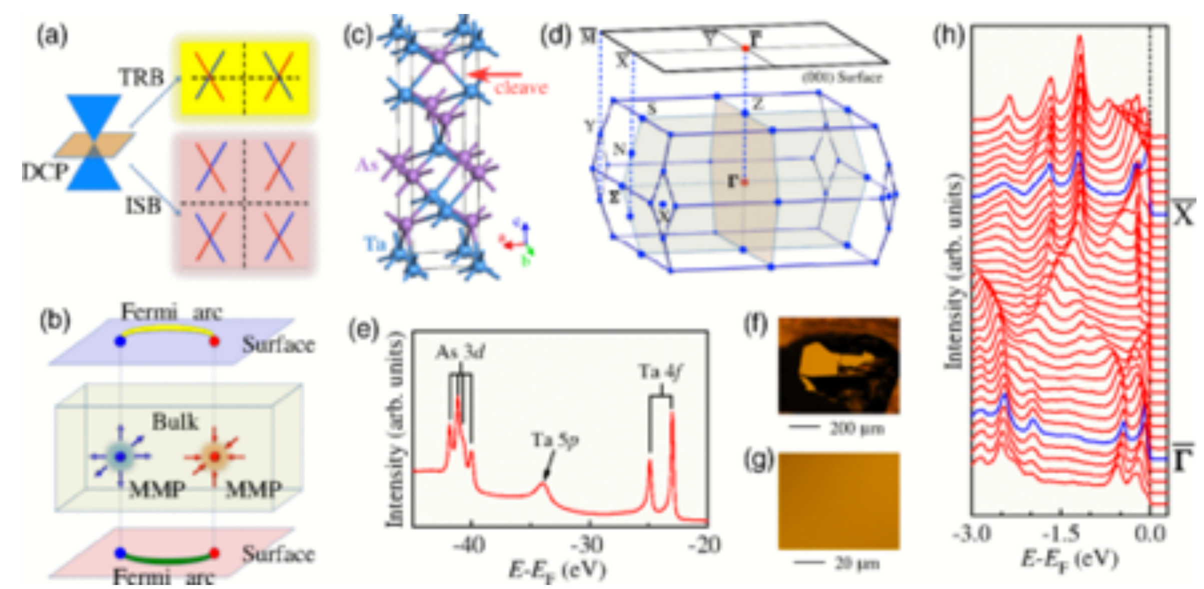

复旦大学
FUDAN UNIVERSITY

Extensions

Type-II Weyl semimetal

Hybrid Weyl semimetal

Dirac fermion, type-II Dirac nodes

nodal line semimetal

hourglass fermion

new fermion…….

Part 1 Topological magnons: the case of Weyl magnon

2. Antiferromagnets and spin wave excitations

FUDAN UNIVERSITY 1905 復旦大學 FUDAN UNIVERSITY

Ordered AFMs

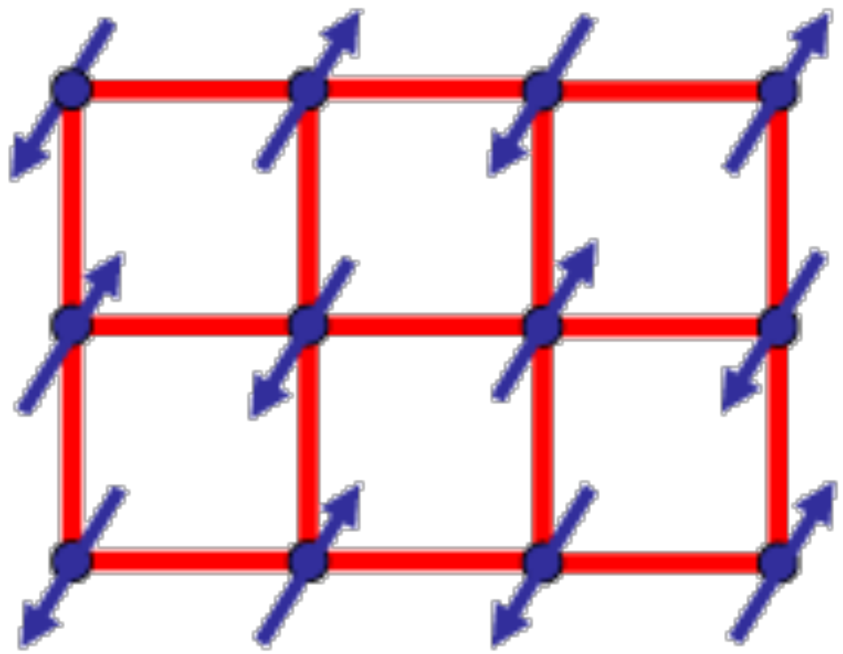

Neel state

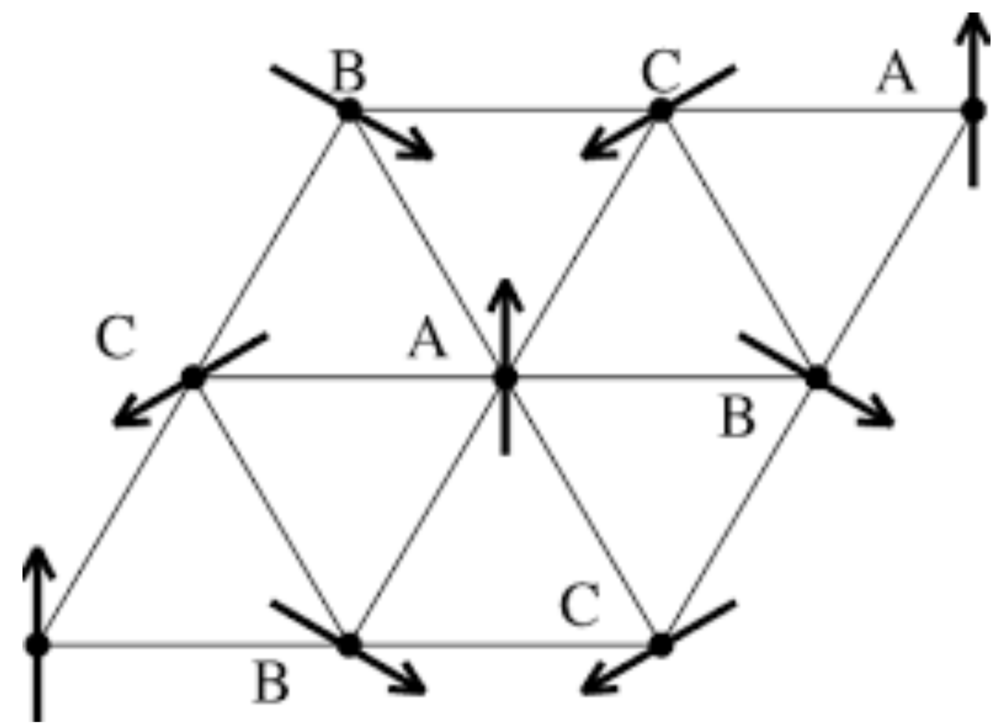

Ground state orders for AFMagnetic Heisenberg model.

Most known magnets are antiferromagnets.

复旦大學

FUDAN UNIVERSITY

Propagating spin waves
and
Holstein-Primakoff spin wave

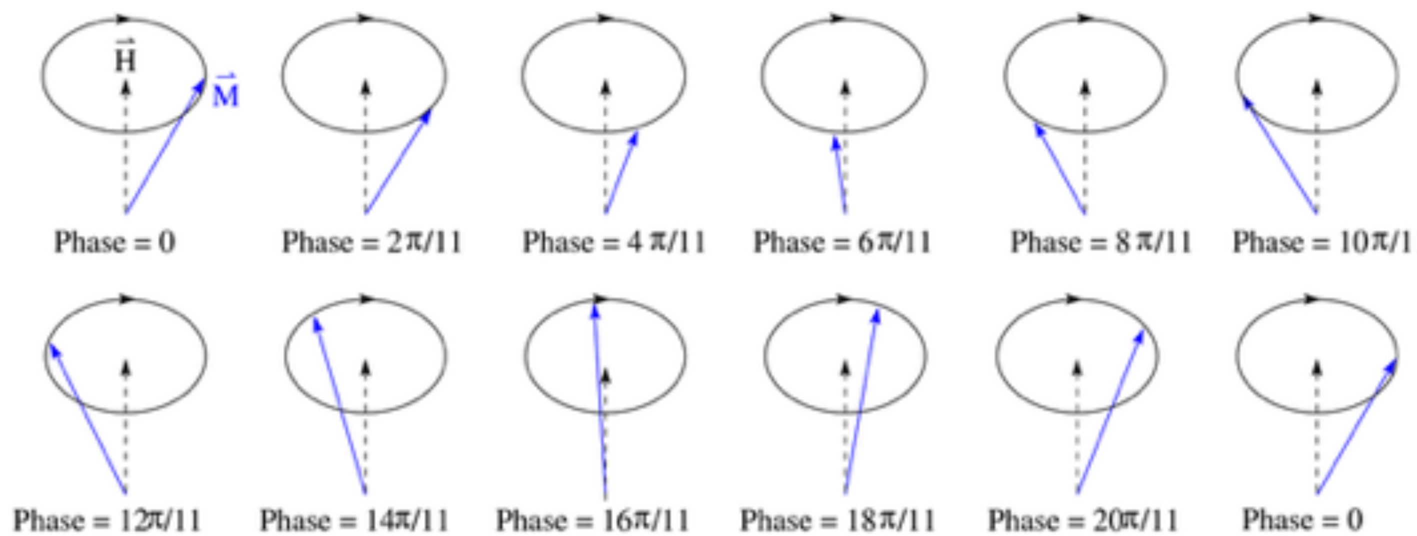

$$S_+ = \hbar\sqrt{2s}\sqrt{1-\frac{a^\dagger a}{2s}}\,a\,, \qquad S_- = \hbar\sqrt{2s}a^\dagger\sqrt{1-\frac{a^\dagger a}{2s}}\,, \qquad S_z = \hbar(s-a^\dagger a)\,.$$

Spin wave excitations in ordered AFM: Pyrochlore $Yb_2Ti_2O_7$

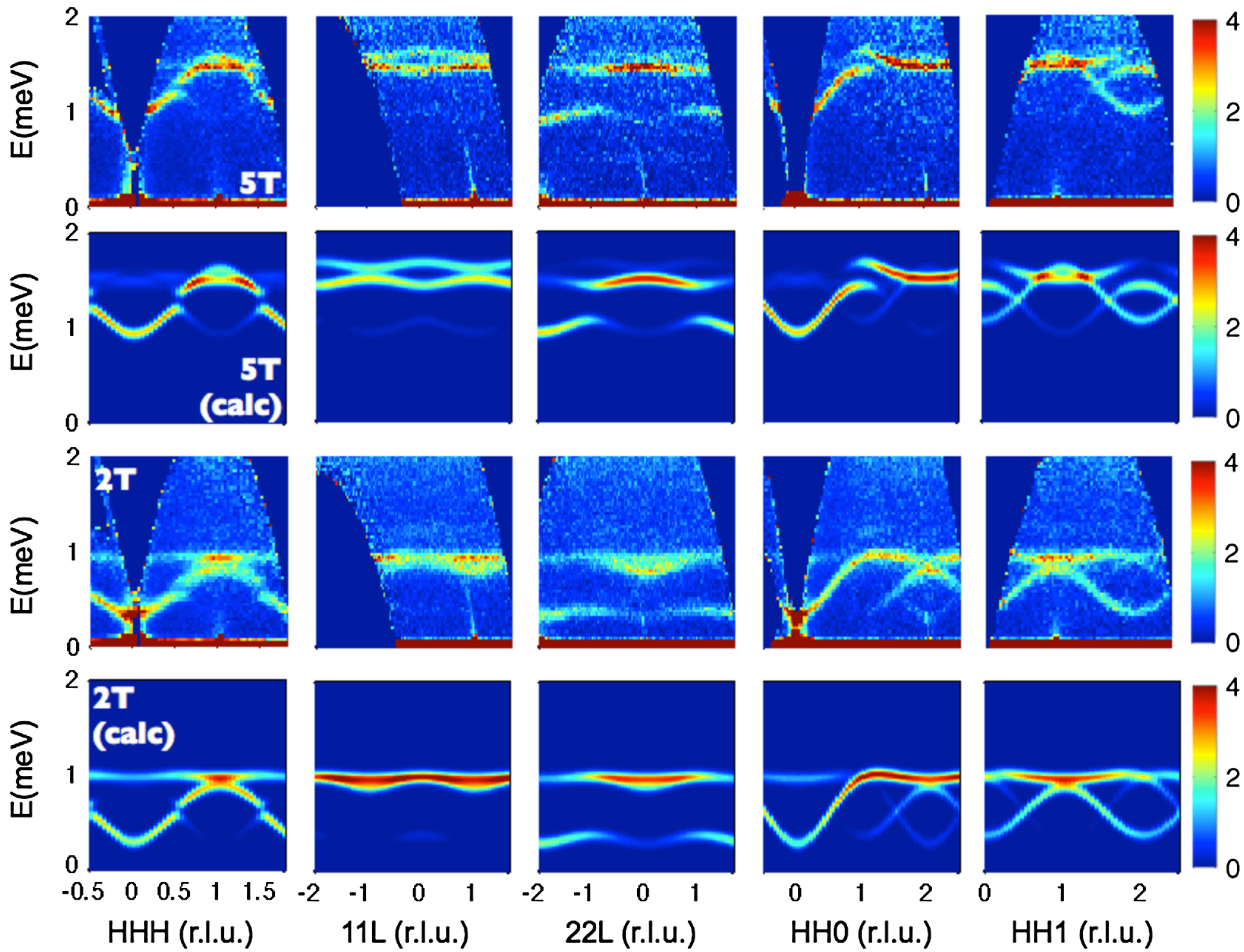

Kate A. Ross,[1] Lucile Savary,[2] Bruce D. Gaulin,[1,3,4] and Leon Balents[5,*]

PHYSICAL REVIEW X **1**, 021002 (2011)

Part 1 Topological magnons: the case of Weyl magnon

3. Weyl magnons: uniqueness and extension

Remark

Weyl band touching is a topological property of the band structure, and is thus **independent** from the particle statistics.

It can be fermion, e.g. electron, can also be boson, e.g. photon.

类似于 breathing

Breathing Pyrochlore

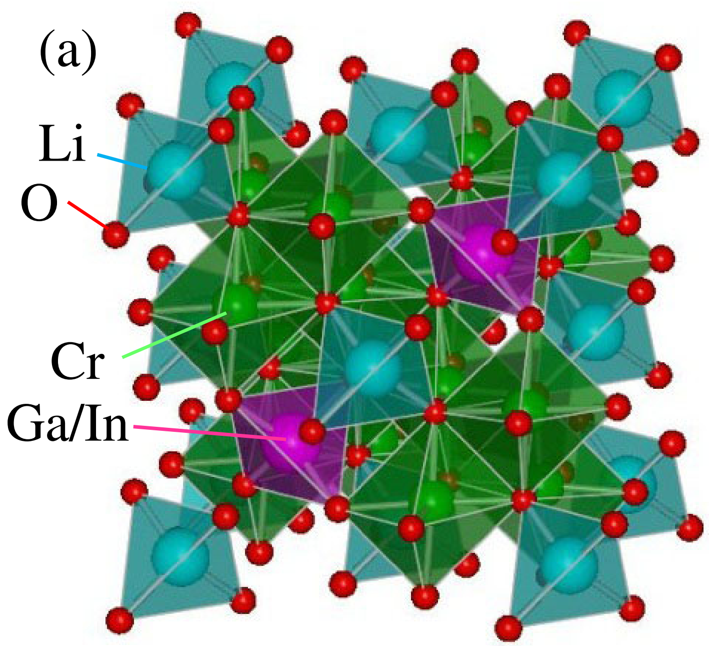

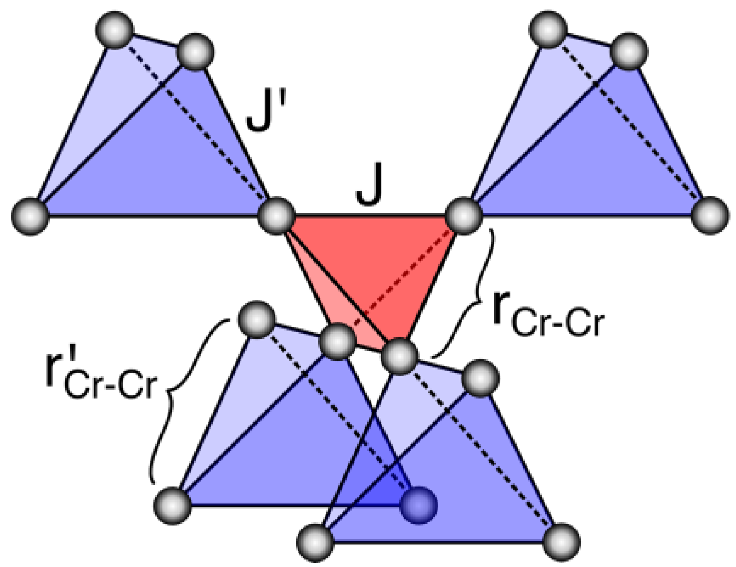

Breathing Pyrochlore

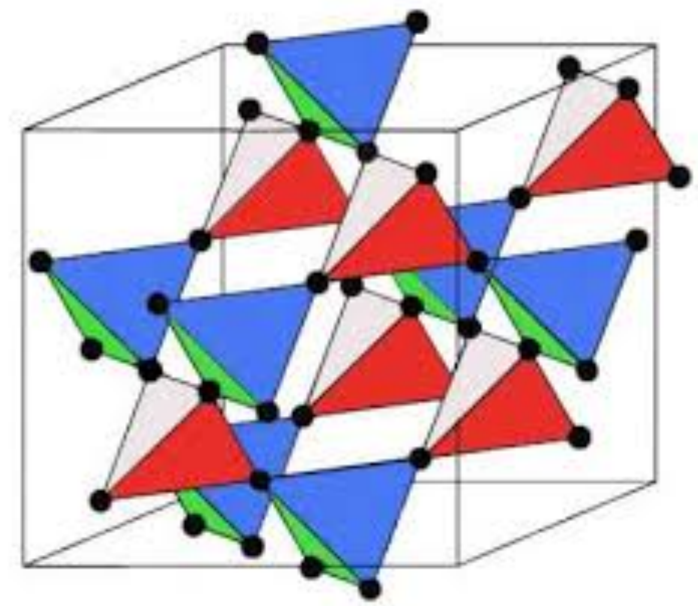

Regular Pyrochlore

K. Kimura, S. Nakatsuji, and T. Kimura, **PhysRevB** 2014,
Yoshihiko Okamoto, Gøran J. Nilsen, J. Paul Attfield, and Zenji Hiroi, **PhysRevLett** 2013,
Yu Tanaka, Makoto Yoshida, Masashi Takigawa, Yoshi- hiko Okamoto, and Zenji Hiroi, **PhysRevLett** 2014.

Minimal model and ground states

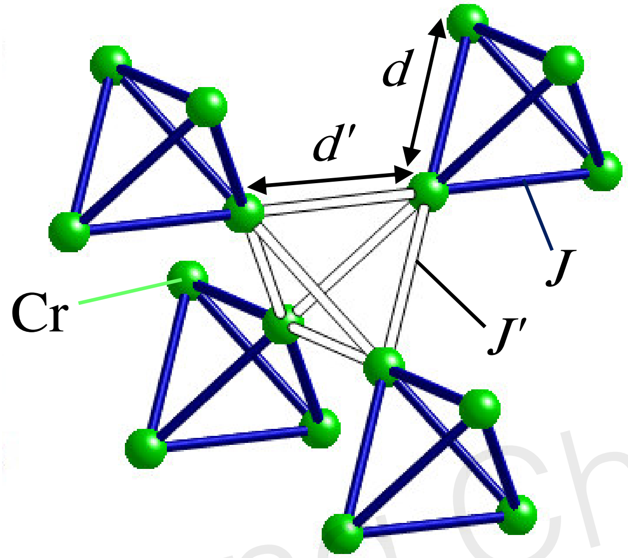

As there is no orbital degeneracy for the $3d^3$ electron configuration of Cr^{3+} ions, the orbital angular momentum is fully quenched and the Cr^{3+} local moment is well described by the total spin $S = 3/2$ via the Hund's rule. As

$$H = J \sum_{\langle ij \rangle \in \mathrm{u}} \mathbf{S}_i \cdot \mathbf{S}_j + J' \sum_{\langle ij \rangle \in \mathrm{d}} \mathbf{S}_i \cdot \mathbf{S}_j + D \sum_i (\mathbf{S}_i \cdot \hat{z}_i)^2 ,$$

Treating spins as classical vectors, simple algebra gives some rules for ground states

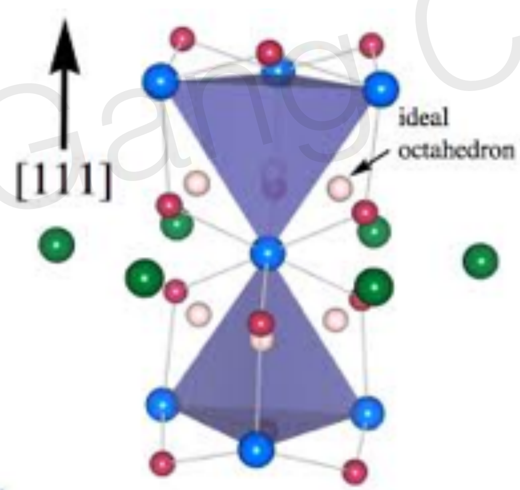

$$\sum_{\langle ij \rangle \in \mathrm{u}} \mathbf{S}_i \cdot \mathbf{S}_j \sim \frac{1}{2} \Big(\sum_{i \in \mathrm{u}} \mathbf{S}_i \Big)^2$$

$$\sum_{\langle ij \rangle \in \mathrm{d}} \mathbf{S}_i \cdot \mathbf{S}_j \sim \frac{1}{2} \Big(\sum_{i \in \mathrm{d}} \mathbf{S}_i \Big)^2$$

复旦大学
FUDAN UNIVERSITY

Phase diagram

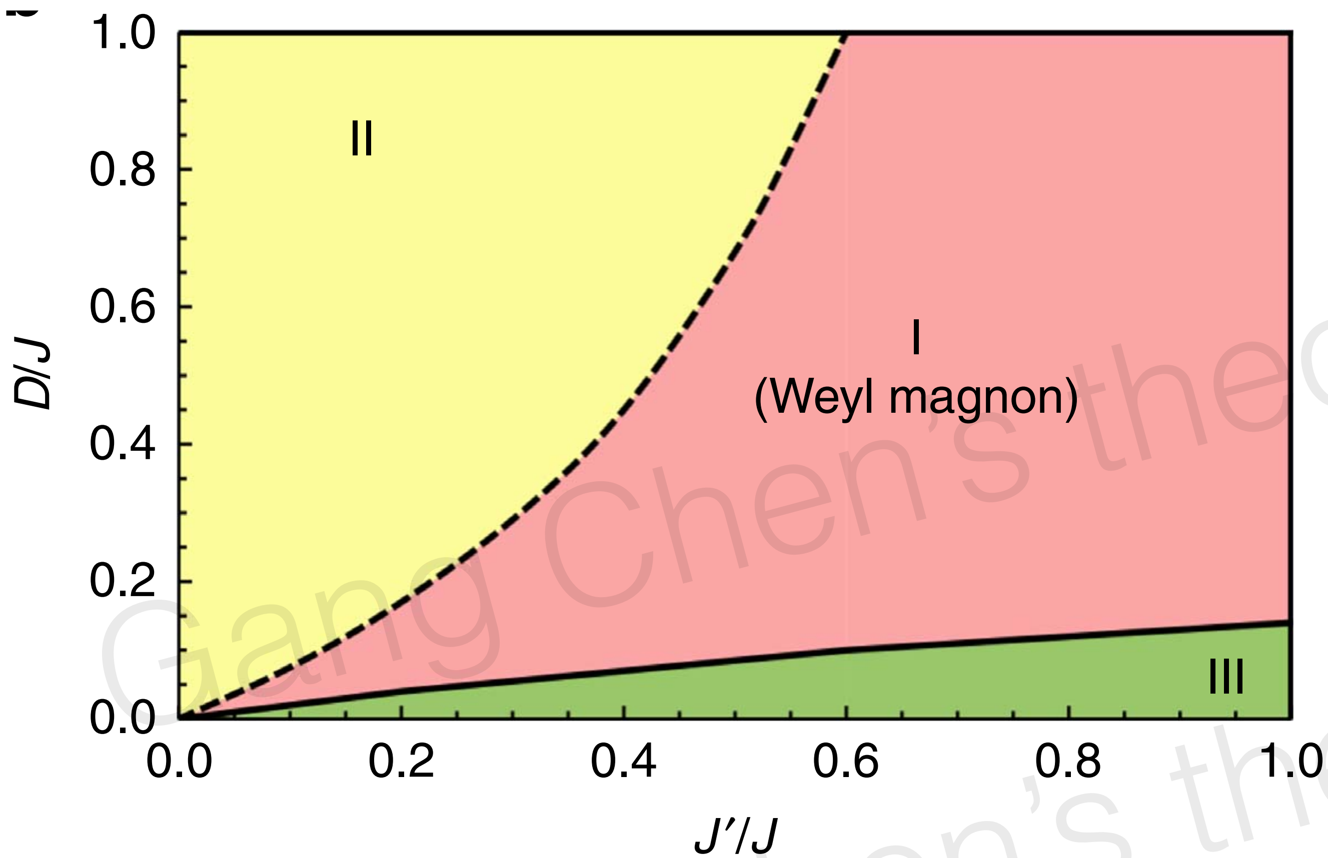

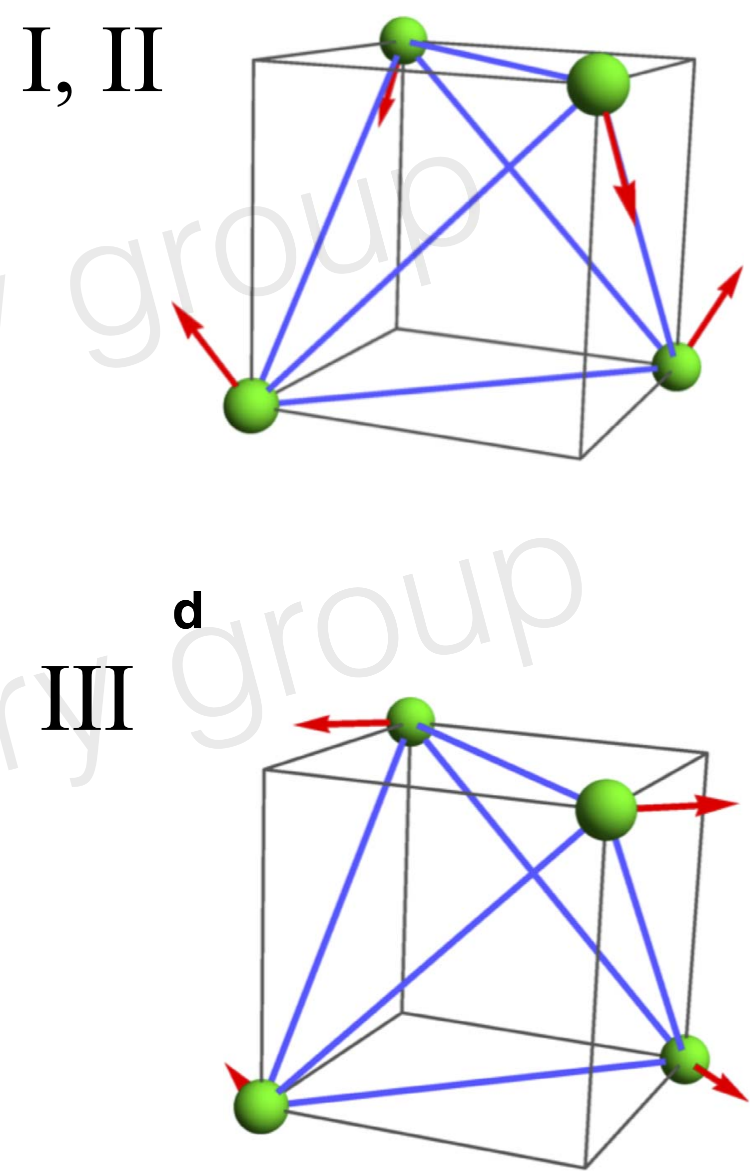

I,II have the same order,
but are distinct **topologically**!

Quantum order by disorder

$$\mathbf{S}_i^{\mathrm{cl}} \equiv S\hat{m}_i = S(\cos\theta\,\hat{x}_i + \sin\theta\,\hat{y}_i),$$

Holstein-Primarkoff bosons to express the spin operators as $\mathbf{S}_i \cdot \hat{m}_i = S - a_i^\dagger a_i$, $\mathbf{S}_i \cdot \hat{z}_i = (2S)^{1/2}(a_i + a_i^\dagger)/2$, and $\mathbf{S}_i \cdot (\hat{m}_i \times \hat{z}_i) = (2S)^{1/2}(a_i - a_i^\dagger)/(2i)$. Keeping terms in

I,II

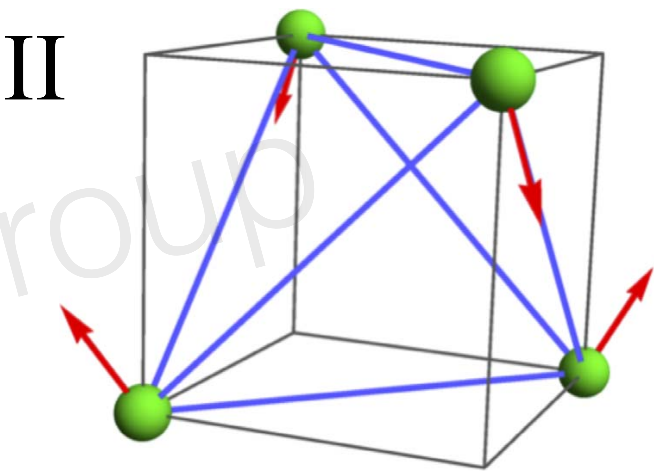

a

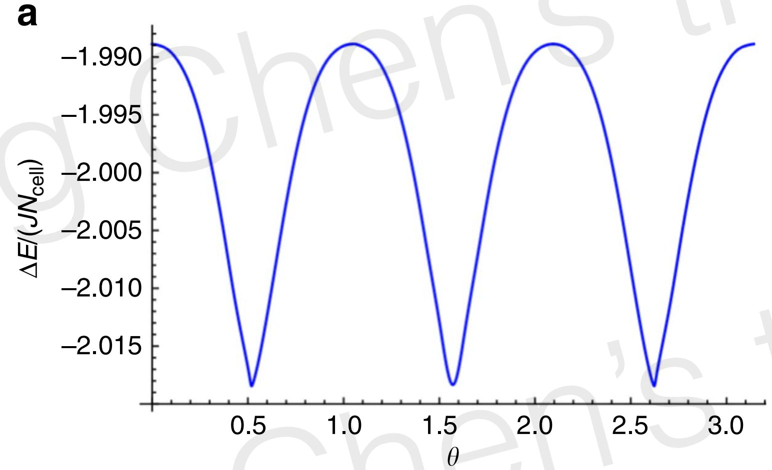

d

III

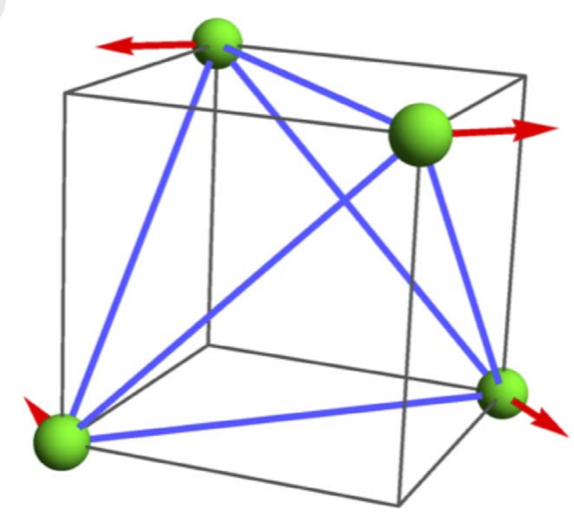

c

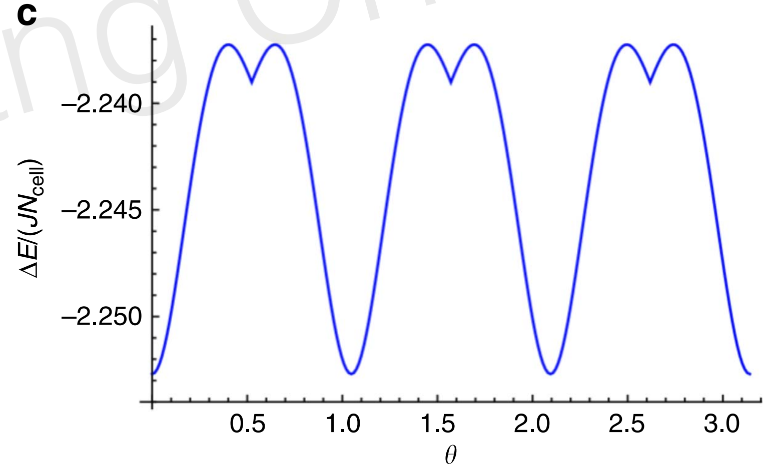

Weyl magnons

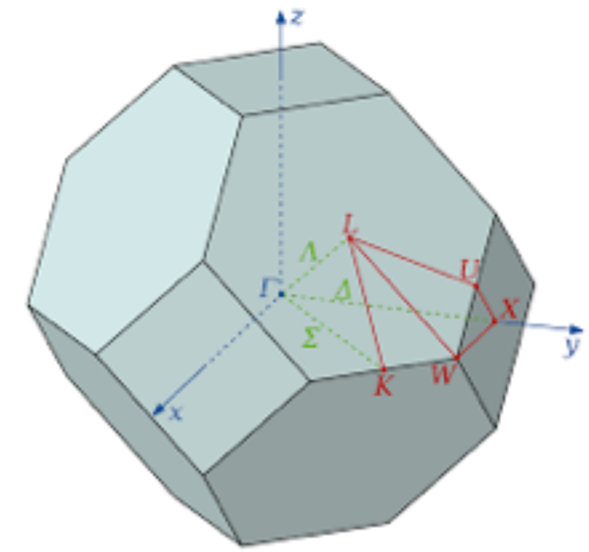

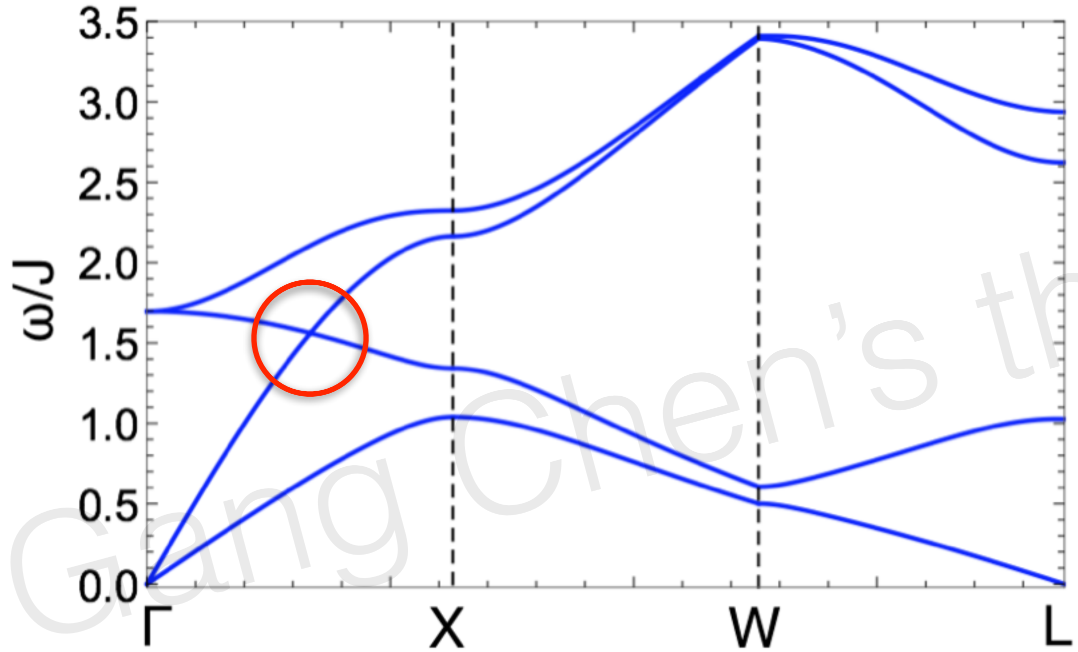

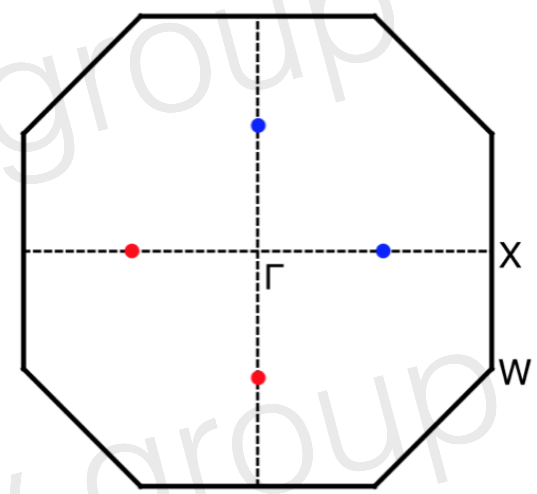

surface arc states

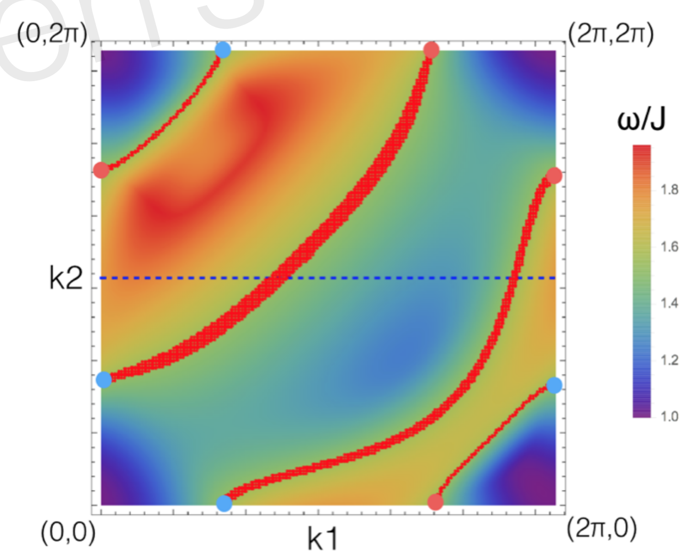

(a)

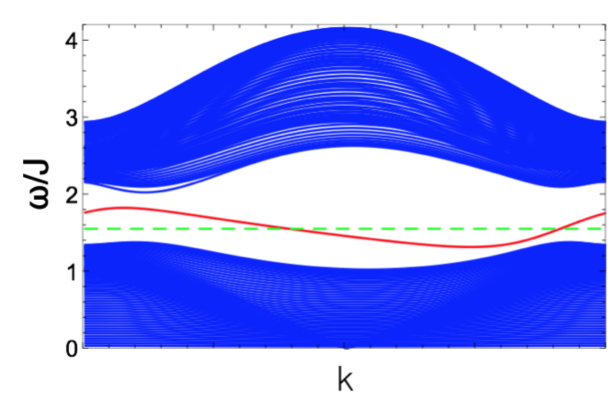

(b)

Tune Weyl nodes with magnetic field

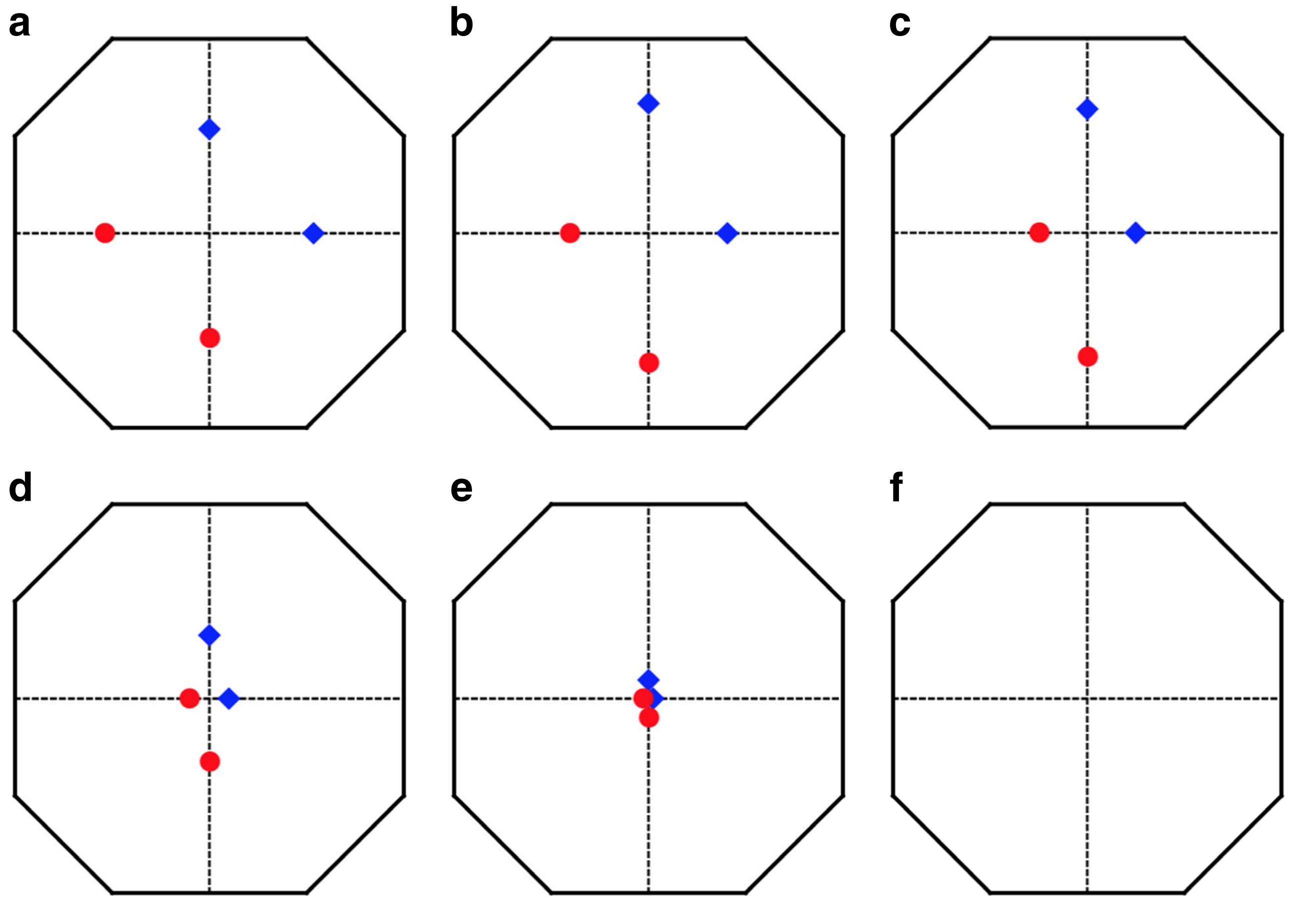

Figure 5 | The evolution of Weyl nodes under the magnetic field. Applying a magnetic field along the global z direction, $\mathbf{B}=B\hat{\mathbf{z}}$, Weyl nodes are shifted but still in $k_z=0$ plane. They are annihilated at Γ when magnetic field is strong enough. Red and blue indicate the opposite chirality. (**a**,**f**): $B=0$, $0.1J$, $0.5J$, $0.9J$, $1.0J$, $1.1J$. We have set $D=0.2J$, $J'=0.6J$ and $\theta=\pi/2$.

different from Weyl electrons

How to probe in a REAL experiment?

1. Neutron scattering: detect the Weyl nodes as well as the consequence (the surface arc states that connect the Weyl nodes).

2. Thermal Hall effect: magnon Weyl nodes contribute the thermal currents that are tunable by external magnetic field.

3. Optically: as Weyl node must appear at finite energy, one needs to use pump-probe measurement.

COMPARE TO Weyl fermion in the electron system

復旦大學 FUDAN UNIVERSITY

Extension

Dirac magnons (Yuan Li, Chen Fang, Jingsheng Wen)
vs
Dirac electron

nodal line magnon (??)
vs
nodal line semimetal

Magnon topological insulator (Schnyder, Katsura)
vs
electron topological insulator

Summary

Band topology of magnon can be another interesting thing to look at among these magnetically ordered systems.

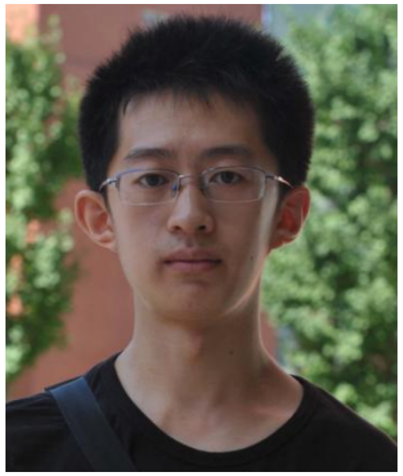

Fei-Ye Li
(Fudan)

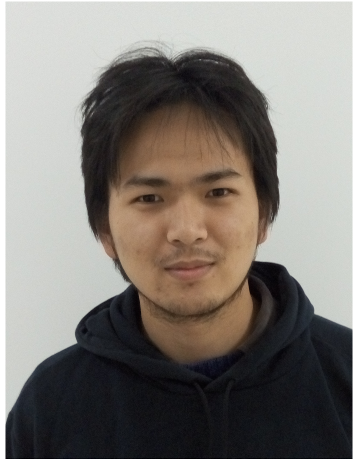

Yaodong Li
(Fudan->UCSB)

and Yue Yu, Leon Balents,
YongBaek Kim,
Arun Paramekanti

Fei-Ye Li, Yao-dong Li, YB Kim, L Balents, Yue Yu, **Gang Chen***, Nature Comms. 7, 12691 (2018)
Fei-Ye Li, Yao-dong Li, Yue Yu, A Paramekanti, **Gang Chen*,** Phys. Rev. B, 95, 085132 (2017)

復旦大學
FUDAN UNIVERSITY

Part 2 Detecting hidden multipolar orders in quantum magnets

1. **Hidden orders in condensed matter physics**

we undertand the order/structure,

we know how thing work, function
make prediction

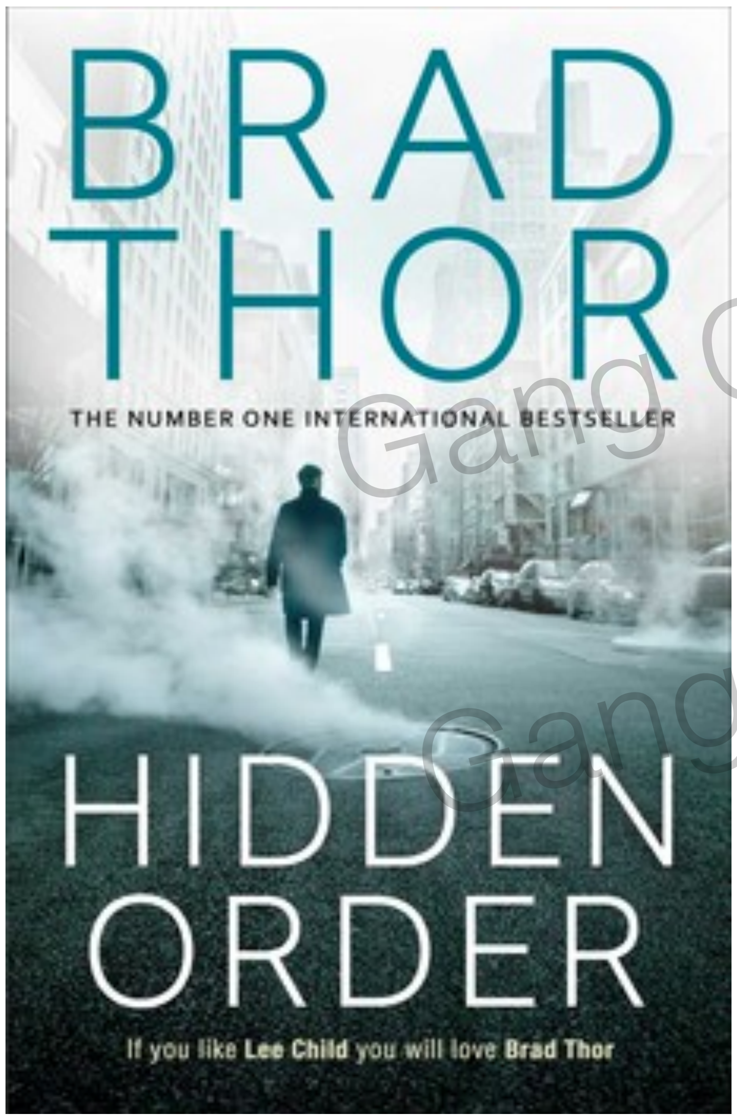

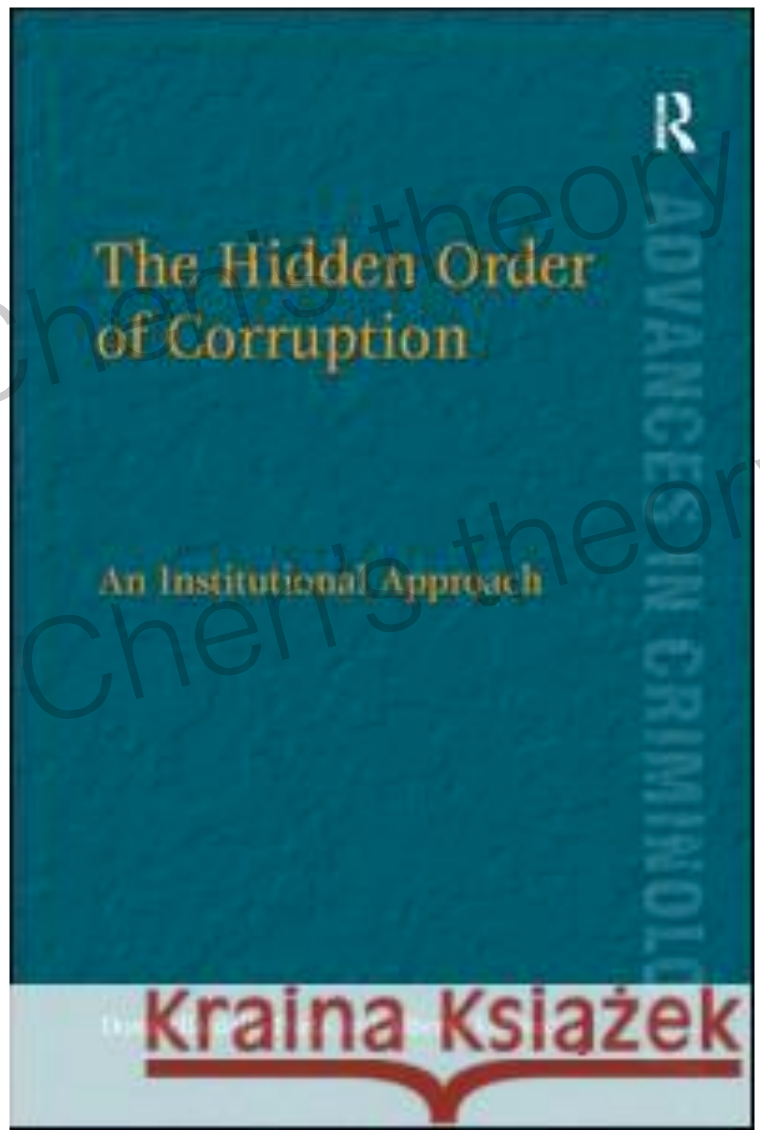

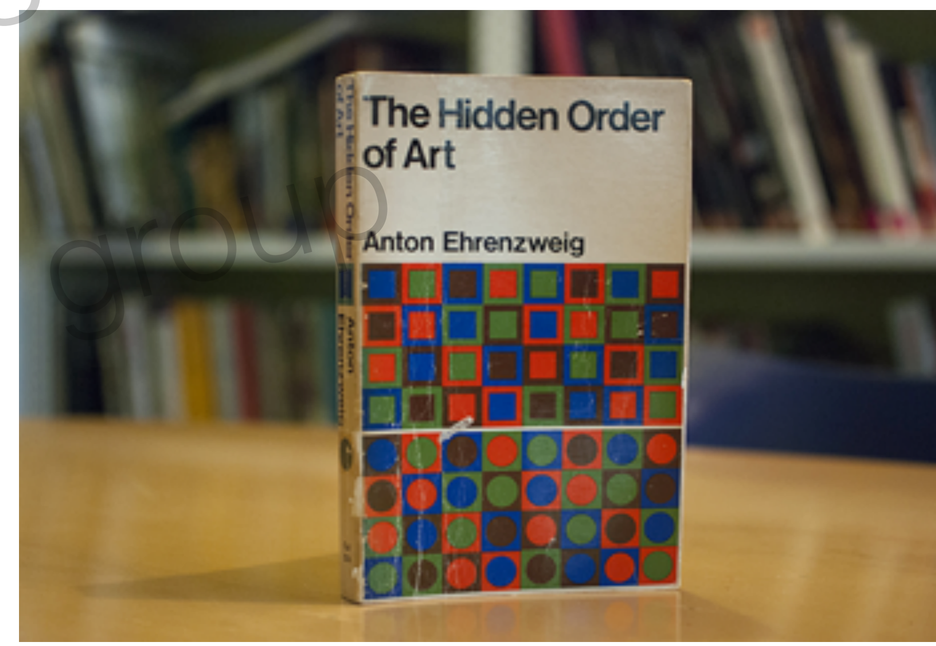

Hidden order in condensed matter

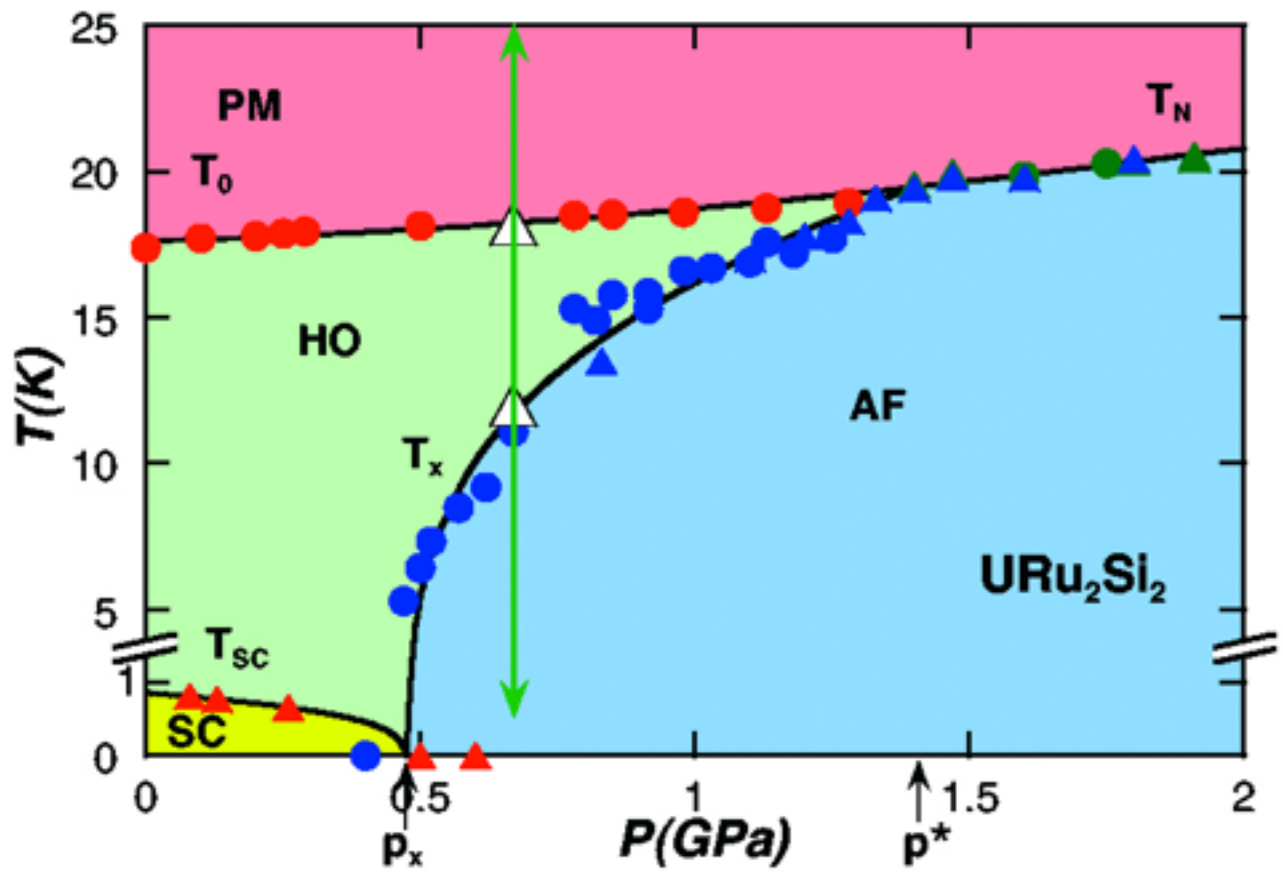

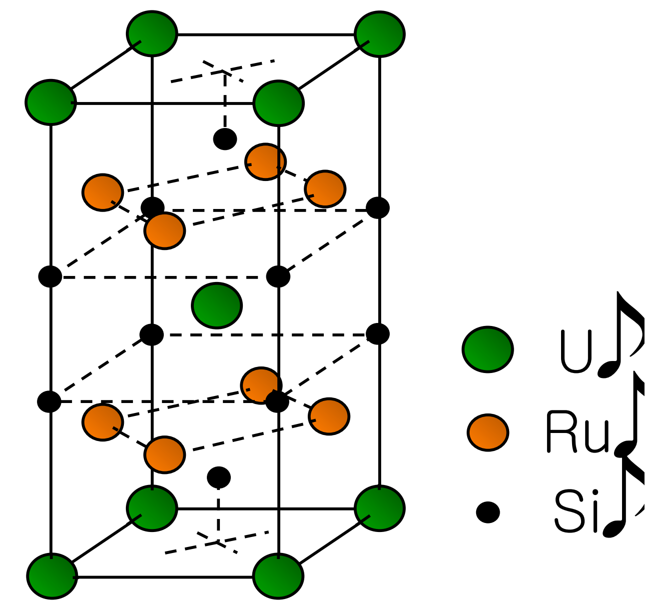

- Hidden order: “dark matter” in CMT
- URu_2Si_2
  - Second order transition at ~17K, $\Delta S \sim 0.42$ Rln2
  - Order parameters unknown after decades

Nature of hidden orders

1. Magnetic multipolar order
   Quadrupolar order
   Octupolar order

2. Electric multipolar order

3. Orbital order

…

How to probe these hidden orders?

Part 2 Detecting hidden multipolar orders in quantum magnets

2. **Hidden orders with intertwined multipolar structure in rare-earth magnets**

A rare-earth triangular lattice quantum spin liquid: **$YbMgGaO_4$**

collaboration with QM Zhang, Jun Zhao, Yuesheng Li, Yaodong Li

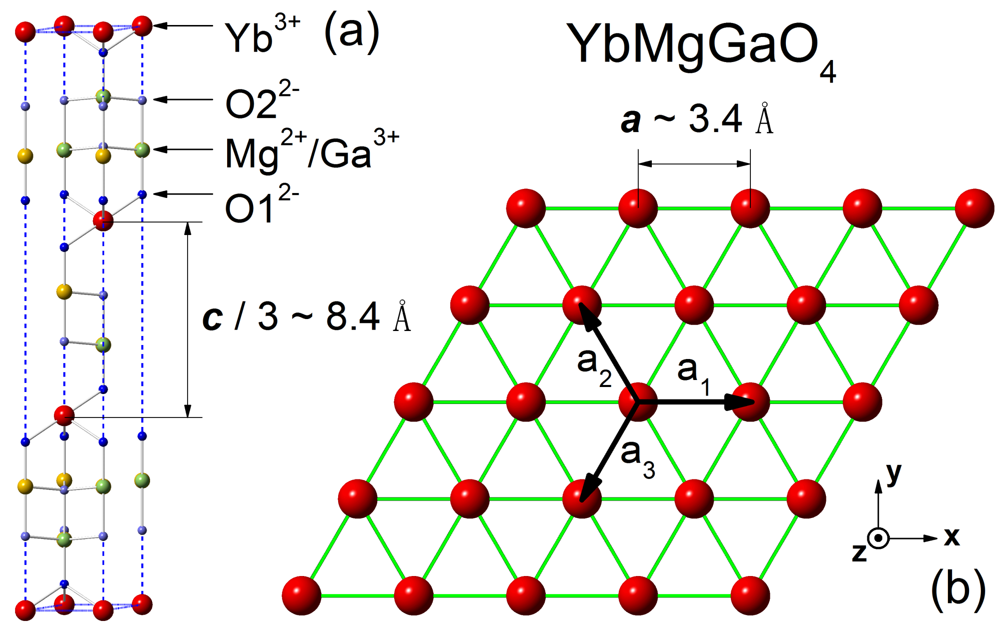

Qingming Zhang
(Renmin)

- Hastings-Oshikawa-Lieb-Shultz-Mattis theorem.
- Recent extension to spin-orbit coupled insulators (Watanabe, Po, Vishwanath, Zaletel, PNAS 2015).
- This is likely the **first strong spin-orbit coupled QSL with odd electron filling** and effective spin-1/2.
- It is the first clear observation of $T^{2/3}$ heat capacity. (needs comment.)
- Inelastic neutron scattering is consistent with spinon Fermi surface results.
- We think it is a spinon Fermi surface U(1) QSL.

Inelastic neutron scattering performed by Jun Zhao's group and M Mourigal's group

YMGO is not alone: **lots of isostructural materials**

Compound	Magnetic ion	Space group	Local moment	Θ_{CW} (K)	Magnetic transition	Frustration para. f	Refs.
$YbMgGaO_4$	$Yb^{3+}(4f^{13})$	$R\bar{3}m$	Kramers doublet	-4	PM down to 60 mK	$f > 66$	[4]
$CeCd_3P_3$	$Ce^{3+}(4f^{1})$	$P6_3/mmc$	Kramers doublet	-60	PM down to 0.48 K	$f > 200$	[5]
$CeZn_3P_3$	$Ce^{3+}(4f^{1})$	$P6_3/mmc$	Kramers doublet	-6.6	AFM order at 0.8 K	$f = 8.2$	[7]
$CeZn_3As_3$	$Ce^{3+}(4f^{1})$	$P6_3/mmc$	Kramers doublet	-62	Unknown	Unknown	[8]
$PrZn_3As_3$	$Pr^{3+}(4f^{2})$	$P6_3/mmc$	Non-Kramers doublet	-18	Unknown	Unknown	[8]
$NdZn_3As_3$	$Nd^{3+}(4f^{3})$	$P6_3/mmc$	Kramers doublet	-11	Unknown	Unknown	[8]

YD Li, XQ Wang, GC*, PRB 94, 035107 (2016)

Magnetism in the $KBaRE(BO_3)_2$ (RE=Sm, Eu, Gd, Tb, Dy, Ho, Er, Tm, Yb, Lu) series: materials with a triangular rare earth lattice

M. B. Sanders, F. A. Cevallos, R. J. Cava
Department of Chemistry, Princeton University, Princeton, New Jersey 08544

Many ternary chalcogenides $NaRES_2$, $NaRESe_2$, $KRES_2$, $KRESe_2$, $KRETe_2$, $RbRES_2$, $RbRESe_2$, $RbRETe_2$, $CsRES_2$, $CsRESe_2$, etc.)

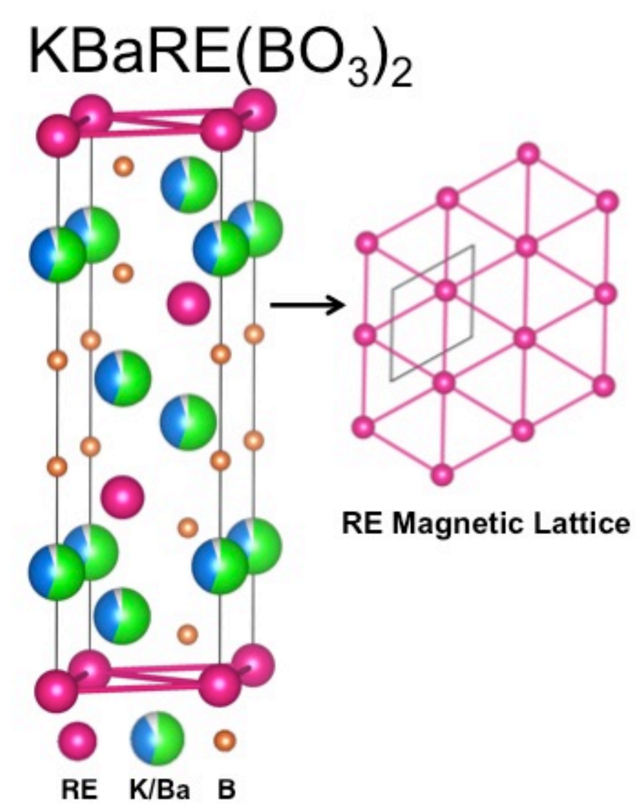

C Liu, YD Li, GC*, PRB 98, 045119 (2018)

Model Hamiltonian for all cases

CHANGLE LIU, YAO-DONG LI, AND GANG CHEN PHYSICAL REVI

TABLE I. The relevant spin Hamiltonians for three different doublets on the triangular lattice. The models for th
and the dipole-octupole doublet have been obtained in the previous works.

Local doublets	The nearest-neighbor spin Hamiltonians on the triangular lattice
Usual Kramers doublet	$H = \sum_{\langle ij \rangle} J_{zz} S_i^z S_j^z + J_{\pm}(S_i^+ S_j^- + S_i^- S_j^+) + J_{\pm\pm}(\gamma_{ij} S_i^+ S_j^+ + \gamma_{ij}^* S_i^- S_j^-) - \frac{i J_{z\pm}}{2} [(\gamma_{ij}^* S_i^+ - \gamma_{ij} S_i^-) S_j^z + S_i^z (\gamma_{ij}^* S_j^+ - \gamma_{ij} S_j^-)]$
Dipole-octupole doublet	$H = \sum_{\langle ij \rangle} J_z S_i^z S_j^z + J_x S_i^x S_j^x + J_y S_i^y S_j^y + J_{yz}(S_i^z S_j^y + S_i^y S_j^z)$
Non-Kramers doublet	$H = \sum_{\langle ij \rangle} J_{zz} S_i^z S_j^z + J_{\pm}(S_i^+ S_j^- + S_i^- S_j^+) + J_{\pm\pm}(\gamma_{ij} S_i^+ S_j^+ + \gamma_{ij}^* S_i^- S_j^-)$

FUDAN UNIVERSITY 1905 復旦大學 FUDAN UNIVERSITY

Model for non-Kramers doublets

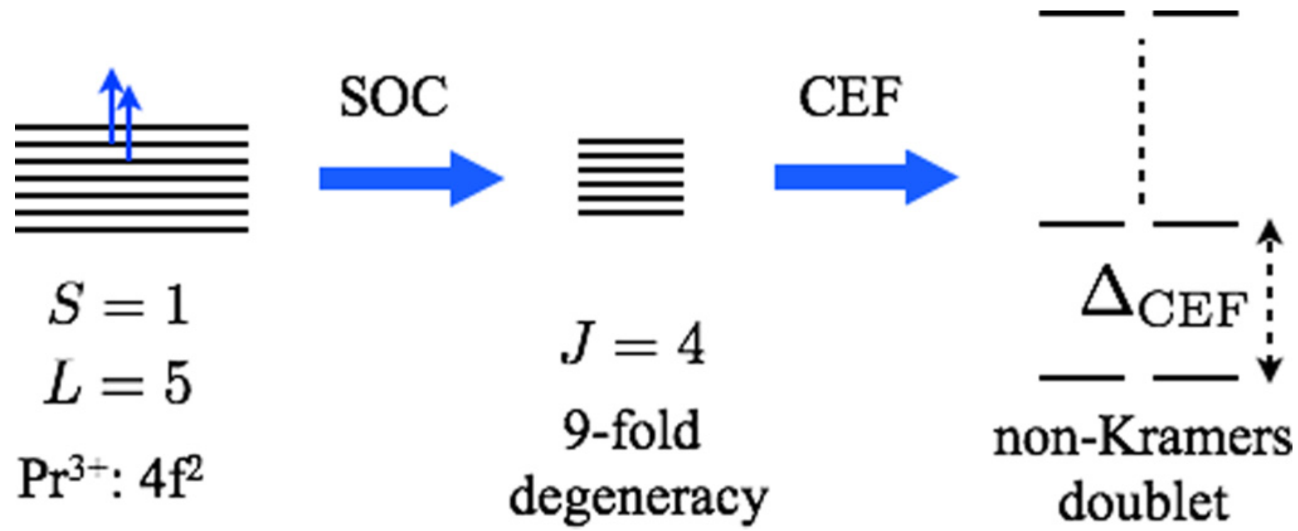

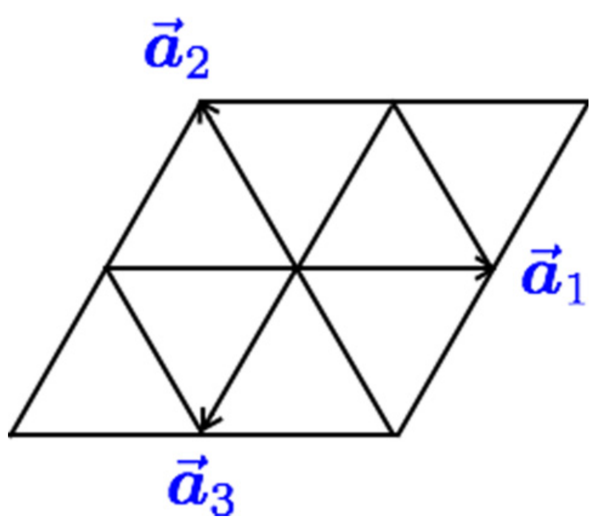

$$H = \sum_{\langle ij \rangle} J_{zz} S_i^z S_j^z + J_{\pm}(S_i^+ S_j^- + S_i^- S_j^+) + J_{\pm\pm}(\gamma_{ij} S_i^+ S_j^+ + \gamma_{ij}^* S_i^- S_j^-), \tag{1}$$

in which, γ_{ij} is a bond-dependent phase factor, and takes 1, $e^{i2\pi/3}$ and $e^{-i2\pi/3}$ on the $\boldsymbol{a}_1, \boldsymbol{a}_2$, and $\boldsymbol{a}_3$ bond (see Fig. 2),

Time reversal symmetry forbids the coupling between transverse and Ising components.

Kitaev interaction

$$
\begin{aligned}
S_i^a &\equiv \sqrt{\frac{2}{3}} S_i^x + \sqrt{\frac{1}{3}} S_i^z, \\
S_i^b &\equiv \sqrt{\frac{2}{3}} \Big(-\frac{1}{2} S_i^x + \frac{\sqrt{3}}{2} S_i^y\Big) + \sqrt{\frac{1}{3}} S_i^z, \\
S_i^c &\equiv \sqrt{\frac{2}{3}} \Big(-\frac{1}{2} S_i^x - \frac{\sqrt{3}}{2} S_i^y\Big) + \sqrt{\frac{1}{3}} S_i^z,
\end{aligned}
$$

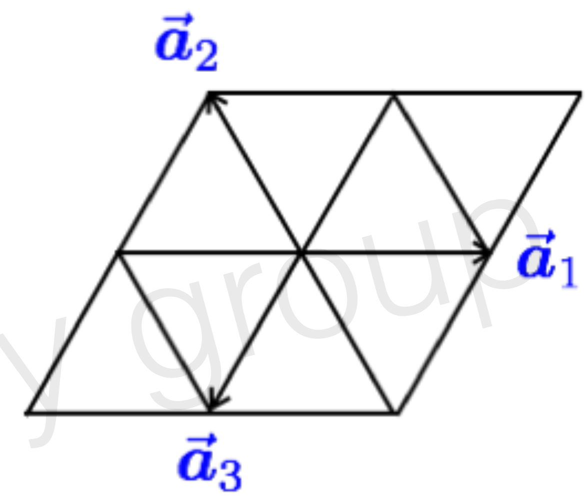

$$
\begin{aligned}
H = \sum_{\langle ij \rangle \in \alpha} \Big[& J \boldsymbol{S}_i \cdot \boldsymbol{S}_j + K S_i^\alpha S_j^\alpha \\
& + \sum_{\beta, \gamma \neq \alpha} \Gamma (S_i^\alpha S_j^\beta + S_i^\beta S_j^\alpha + S_i^\alpha S_j^\gamma + S_i^\gamma S_j^\alpha) \\
& + \sum_{\beta, \gamma \neq \alpha} (K + \Gamma)(S_i^\beta S_j^\gamma + S_i^\gamma S_j^\beta) \Big],
\end{aligned}
$$

Kitaev material beyond iridates: the advantage of f electrons.

pointed out in Fei-Ye Li, YD Li, …, GC, arXiv 2016, PRB 2017

Non-Kramers doublets: intertwined multipolar orders

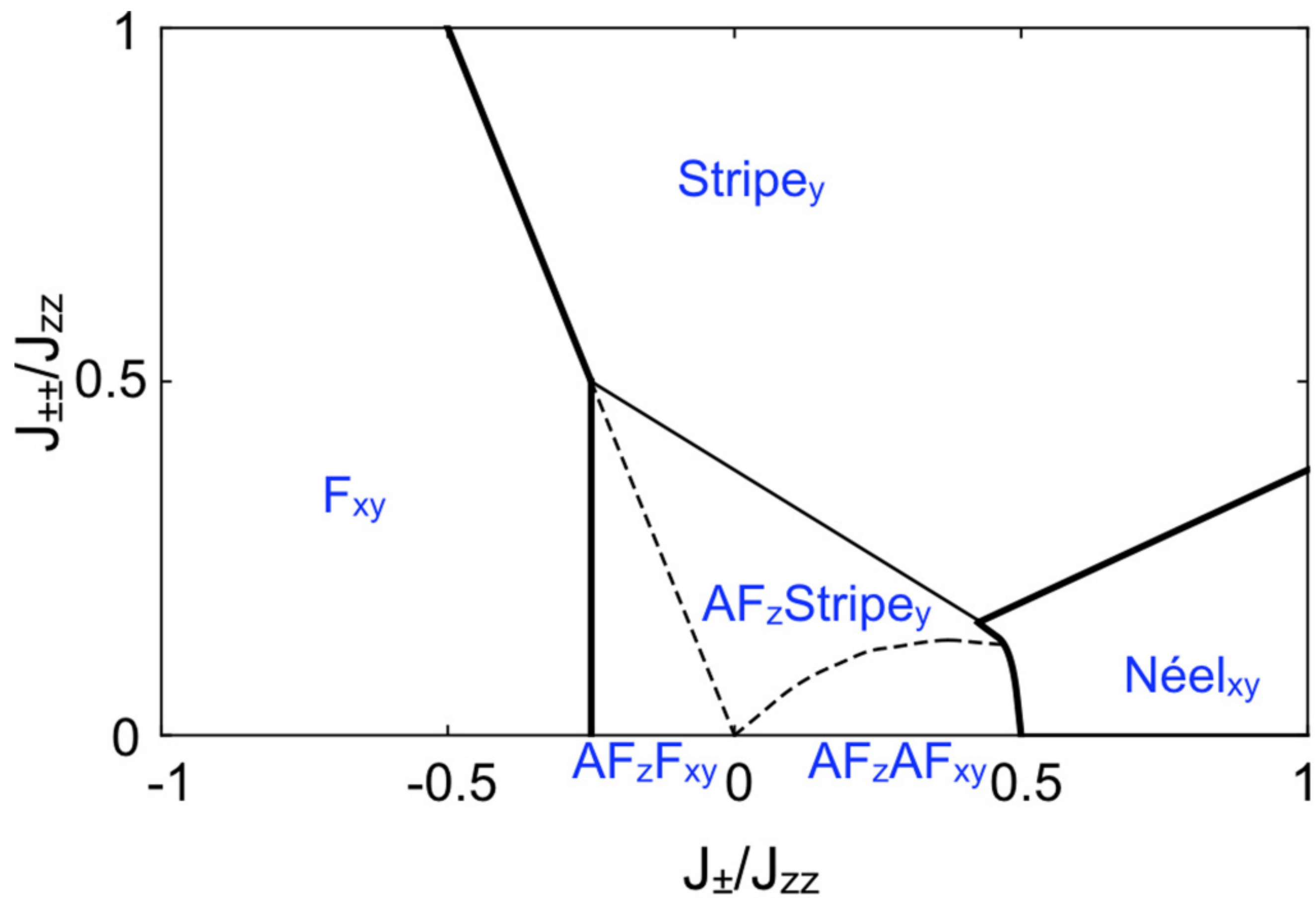

XXZ axis

We first notice that in the model, the spin rotation around the z direction by $\pi/4$ transforms $S^{\pm} \to \mp i S^{\pm}$ and the couplings in the model transform as

$$J_{zz} \to J_{zz}, \quad J_{\pm} \to J_{\pm}, \quad J_{\pm\pm} \to -J_{\pm\pm}. \qquad (2)$$

combined consequence of geometrical frustration
and multipolar nature of the local moments

Non-Kramers doublets: intertwined multipolar orders

TABLE II. The list of ordered phases in the phase diagram of Fig. 3.

States	Order types	Elastic neutron
F_{xy}	pure quadrupolar	no Bragg peak
120° Néel	pure quadrupolar	no Bragg peak
$Stripe_y$	pure quadrupolar	no Bragg peak
AF_zF_{xy}	intertwined multipolar	Bragg peak at K
AF_zAF_{xy}	intertwined multipolar	Bragg peak at K
$AF_zStripe_y$	intertwined multipolar	Bragg peak at K

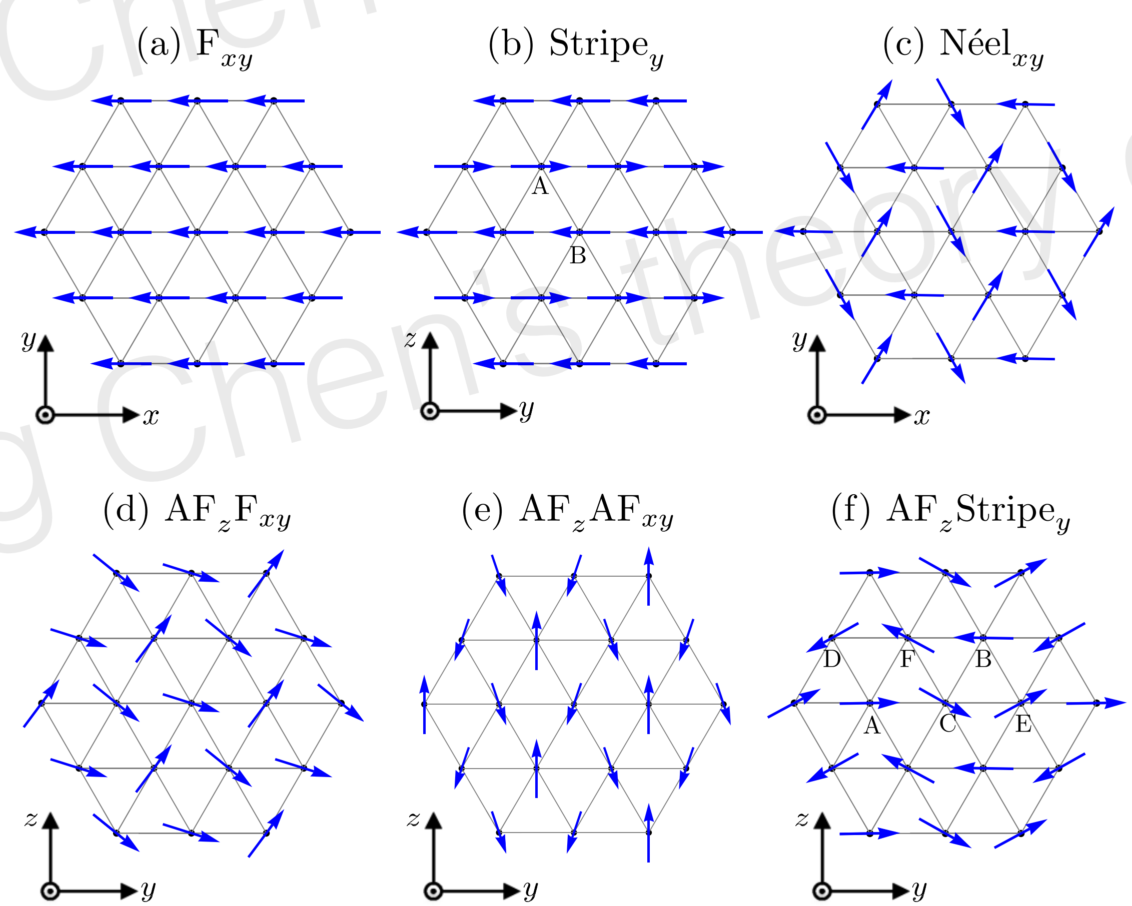

Quantum order by disorder

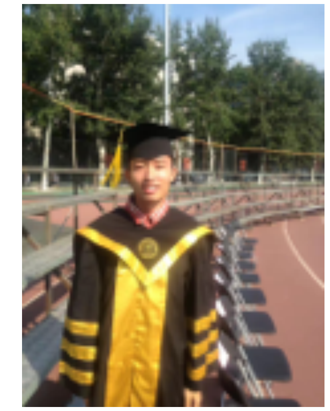

Changle Liu
Fudan

s. Assuming spins with sublattice index s has the direction pointing along the unit vector $\mathbf{n}_s$, one can always associate two unit vectors $\mathbf{u}_s \cdot \mathbf{n}_s = 0$ and $\mathbf{v}_s = \mathbf{n}_s \times \mathbf{u}_s$ so that $\mathbf{n}_s$, $\mathbf{u}_s$ and $\mathbf{v}_s$ are orthogonal with each other. Then we perform Holstein-Primakoff transformation for the spin operator $\mathbf{S}_{\mathbf{r}s}$,

$$\mathbf{n}_s \cdot \mathbf{S}_{\mathbf{r}s} = S - b^\dagger_{\mathbf{r}s} b_{\mathbf{r}s}, \tag{4}$$

$$(\mathbf{u}_s + i\mathbf{v}_s) \cdot \mathbf{S}_{\mathbf{r}s} = (2S - b^\dagger_{\mathbf{r}s} b_{\mathbf{r}s})^{\frac{1}{2}} b_{\mathbf{r}s}, \tag{5}$$

$$(\mathbf{u}_s - i\mathbf{v}_s) \cdot \mathbf{S}_{\mathbf{r}s} = b^\dagger_{\mathbf{r}s} (2S - b^\dagger_{\mathbf{r}s} b_{\mathbf{r}s})^{\frac{1}{2}}. \tag{6}$$

After performing Fourier transformation

$$b_{\mathbf{r}s} = \sqrt{\frac{M}{N}} \sum_{\mathbf{k}\in\overline{\mathrm{BZ}}} b_{\mathbf{k}s} e^{i\mathbf{R}_{\mathbf{r}s}\cdot\mathbf{k}}, \tag{7}$$

the spin Hamiltonian can be rewritten in terms of boson bilinears as

$$H_{\mathrm{sw}} = E_0 + \frac{1}{2} \sum_{\mathbf{k}\in\overline{\mathrm{BZ}}} \left[\Psi(\mathbf{k})^\dagger h(\mathbf{k}) \Psi(\mathbf{k}) - \frac{1}{2} \mathrm{tr}\, h(\mathbf{k}) \right], \tag{8}$$

where E_0 is the mean-field energy,

$$\Psi(\mathbf{k}) = [b_{\mathbf{k}1}, \ldots, b_{\mathbf{k}M}, b^\dagger_{-\mathbf{k}1}, \ldots, b^\dagger_{-\mathbf{k}M}]^T, \tag{9}$$

and $h(\mathbf{k})$ is a $2M \times 2M$ Hermitian matrix, and $\overline{\mathrm{BZ}}$ is the magnetic Brillouin zone. H_{sw} can be diagonalized via a standard Bogoliubov transformation $\Psi(\mathbf{k}) = T_{\mathbf{k}} \Phi(\mathbf{k})$ where

$$\Phi(\mathbf{k}) = [\beta_{\mathbf{k}1}, \ldots, \beta_{\mathbf{k}M}, \beta^\dagger_{-\mathbf{k}1}, \ldots, \beta^\dagger_{-\mathbf{k}M}]^T, \tag{10}$$

and $T_{\mathbf{k}} \in SU(M,M)$. Here $SU(M,M)$ refers to indefinite special unitary group that is defined as [43]

$$SU(M,M) = \{g \in \mathbb{C}_{2M\times 2M} : g^\dagger \Sigma g = \Sigma, \det g = 1\}, \tag{11}$$

where Σ is the metric tensor and given as

$$\Sigma = \begin{pmatrix} I_{M\times M} & 0 \\ 0 & -I_{M\times M} \end{pmatrix}. \tag{12}$$

It is straightforward to prove that such transformation preserves the boson commutation rules. The diagonalized Hamiltonian reads

$$\begin{aligned} H_{\mathrm{sw}} &= E_0 + \frac{1}{2} \sum_{\mathbf{k}\in\overline{\mathrm{BZ}}} \left[\Phi(\mathbf{k})^\dagger E(\mathbf{k}) \Phi(\mathbf{k}) - \frac{1}{2} \mathrm{tr}\, h(\mathbf{k}) \right] \\ &= E_0 + E_r + \sum_{\mathbf{k}\in\overline{\mathrm{BZ}}} \omega_{\mathbf{k}s} \beta^\dagger_{\mathbf{k}s} \beta_{\mathbf{k}s}, \end{aligned} \tag{13}$$

where $E(\mathbf{k}) = \mathrm{diag}[\omega_{\mathbf{k}1}, \ldots, \omega_{\mathbf{k}M}, \omega_{-\mathbf{k}1}, \ldots, \omega_{-\mathbf{k}M}]$ and

$$E_r = \frac{1}{4} \sum_{\mathbf{k}\in\overline{\mathrm{BZ}}} \mathrm{tr}\,[E(\mathbf{k}) - h(\mathbf{k})] \tag{14}$$

Quantum order by disorder

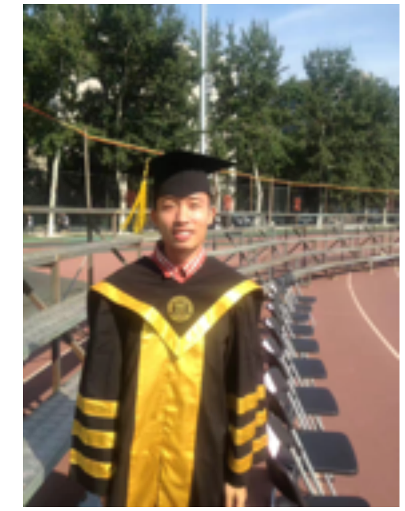

Changle Liu
Fudan

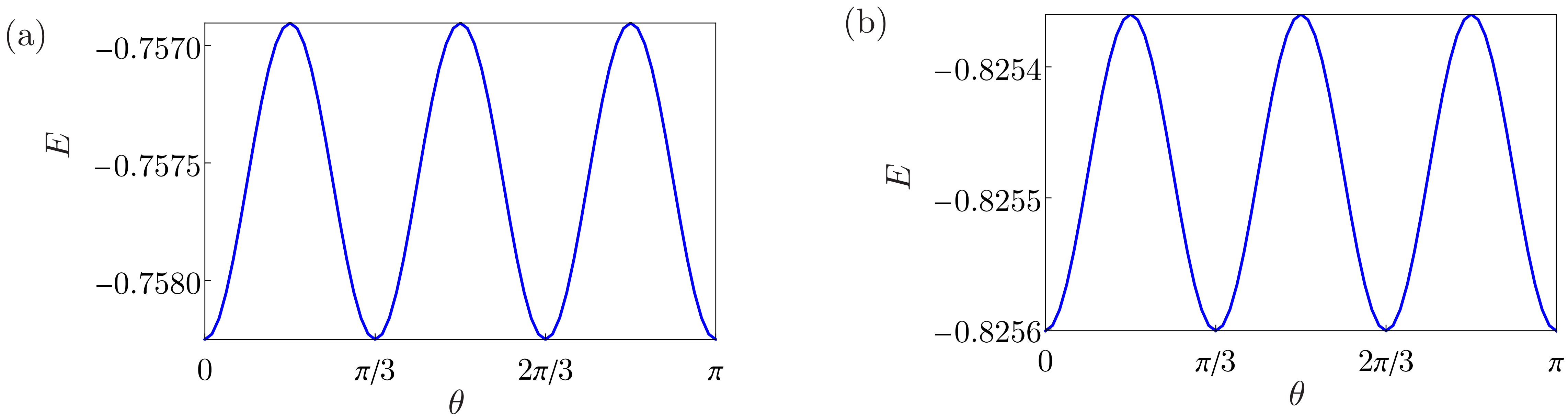

FIG. 5. Energy per spin taking into account quantum zero-point energy vs the azimuth angle θ of spins for (a) the F_{xy} state and (b) the 120° Néel$_{xy}$ state. Here we take the parameter $J_{\pm} = 0.4J_{zz}$, $J_{\pm\pm} = 0.4J_{zz}$ for the F_{xy} state and parameter $J_{\pm} = 0.9J_{zz}$, $J_{\pm\pm} = 0.2J_{zz}$ for the Néel$_{xy}$ state. The zero-point energy is calculated within the linear spin-wave method.

The idea of non-commutative observables

To detect intertwined multipolar orders, one can combine both elastic and inelastic neutron scattering measurements.

$$\mathcal{S}^{zz}(\mathbf{q},\omega > 0) = \frac{1}{2\pi N}\sum_{ij}\int_{-\infty}^{+\infty} \mathrm{d}t\, e^{i\mathbf{q}\cdot(\mathbf{r}_i-\mathbf{r}_j)-i\omega t}\big\langle S_i^z(0)S_j^z(t)\big\rangle.$$

as if one is doing polarized neutron scattering measurements.

FUDAN UNIVERSITY 1905 復旦大學 FUDAN UNIVERSITY

Detection of the intertwined multipolar orders: excitations

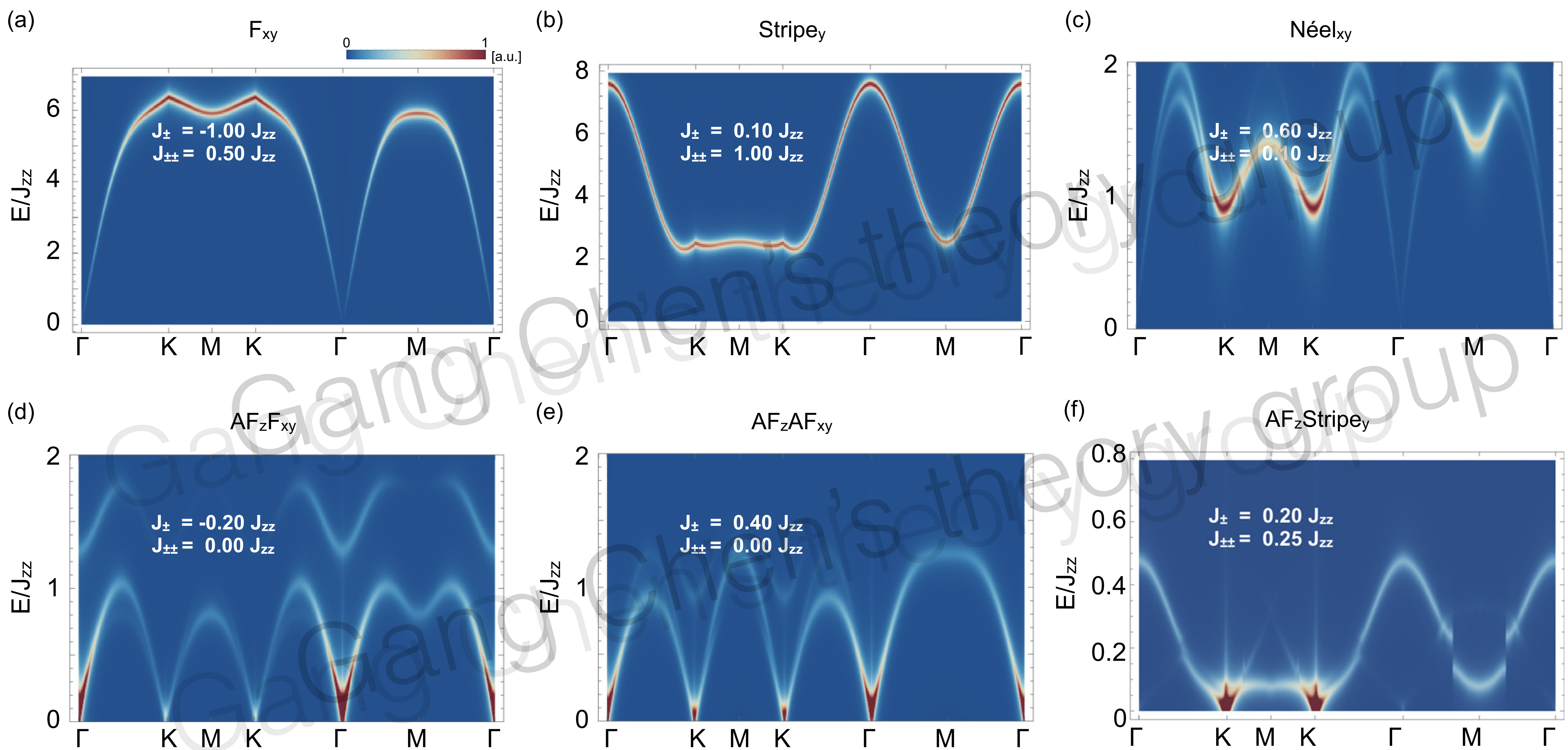

Selection rules

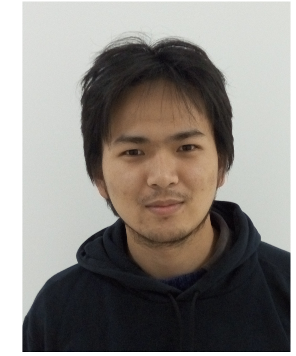

Yaodong Li
Fudan -> UCSB

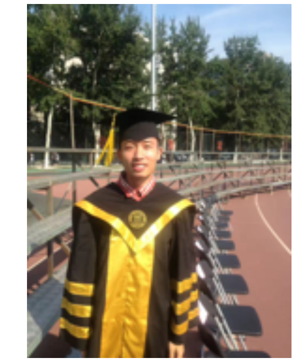

Changle Liu
Fudan

selection rule associated with the symmetry generated by

$$\hat{W} = T_{-\mathbf{a}_1+\mathbf{a}_2} \otimes e^{i\pi \sum_j S_j^z}, \tag{18}$$

where $T_{-\mathbf{a}_1+\mathbf{a}_2}$ denotes the lattice translation by $-\mathbf{a}_1 + \mathbf{a}_2$. The Hamiltonian stays invariant under $\hat{W}$, $[\hat{W}, H] = 0$.

From now on, we introduce the notation s and $\bar{s}$ to denote the sublattice pair that is interchanged under the action of $\hat{W}$. In the labeling of Fig. 4, we find that $\bar{A} = B, \bar{C} = D, \bar{E} = F$.

For the elementary excitations, the effect of $\hat{W}$ is such that

$$\text{Stripe}_y : \hat{W} b_{\mathbf{k},s} \hat{W}^\dagger = e^{i\phi(\mathbf{k})} b_{\mathbf{k},\bar{s}}, s = A, B, \tag{19}$$

$$\text{Stripe}_y\text{AF}_z : \hat{W} b_{\mathbf{k},s} \hat{W}^\dagger = e^{i\phi(\mathbf{k})} b_{\mathbf{k},\bar{s}}, s = A, \ldots, F, \tag{20}$$

where $\phi(\mathbf{k}) = -k_x + k_y$.

The eigenmodes of $\hat{W}$ take bonding/antibonding form,

$$\alpha_{\mathbf{k},s,\pm} = b_{\mathbf{k},s} \pm b_{\mathbf{k},\bar{s}}, \tag{21}$$

whose eigenvalues are

$$\hat{W} \alpha_{\mathbf{k},s,\pm} \hat{W}^\dagger = \pm e^{i\phi(\mathbf{k})} \alpha_{\mathbf{k},s,\pm}. \tag{22}$$

Since $\hat{W}$ is a symmetry of the Hamiltonian, the energy eigenmodes are separate linear combinations of $\alpha_{\mathbf{k},s,\pm}$,

$$\beta_{\mathbf{k},t,\pm} = \sum_s c_{t,s} \alpha_{\mathbf{k},s,\pm} + d_{t,s} \alpha^\dagger_{-\mathbf{k},s,\pm}, \tag{23}$$

and

$$\hat{W} \beta_{\mathbf{k},t,\pm} \hat{W}^\dagger = \pm e^{i\phi(\mathbf{k})} \beta_{\mathbf{k},t,\pm}. \tag{24}$$

The $\pm$ branches do not mix, since they have distinct eigenvalues under $\hat{W}$.

$$S^{zz}(\mathbf{q},\omega > 0) = \sum_n \langle 0| \sum_{s=1} S_s^z(-\mathbf{q}, -\omega)|n\rangle\langle n| \sum_{s=1} S_s^z(\mathbf{q},\omega)|0\rangle$$

$$\propto \sum_n \delta(\omega - (\epsilon_n - \epsilon_0))\langle 0| \sum_{s=1}^{M} (b_{\mathbf{q},s} + b^\dagger_{-\mathbf{q},s})|n\rangle\langle n| \sum_{s=1}^{M} (b_{-\mathbf{q},s} + b^\dagger_{\mathbf{q},s})|0\rangle$$

$$\propto \sum_n \delta(\omega - (\epsilon_n - \epsilon_0))\langle 0| \sum_{s=1}^{M} (\alpha_{\mathbf{q},s,+} + \alpha^\dagger_{-\mathbf{q},s,+})|n\rangle\langle n| \sum_{s=1}^{M} (\alpha_{-\mathbf{q},s,+} + \alpha^\dagger_{\mathbf{q},s,+})|0\rangle.$$

It is thus obvious that the contribution is nonzero if and only if $|n\rangle$ is created by the $\beta_{\mathbf{k},t,+}$ operators. The $\beta_{\mathbf{k},t,-}$ states are not accessible. As a result, the S^z-S^z correlation function only measures coherent excitations with even parity. The odd parity excitations, instead, are present in S^x-S^x and S^y-S^y correlation functions.

Intertwined multipolar order in TmMgGaO4

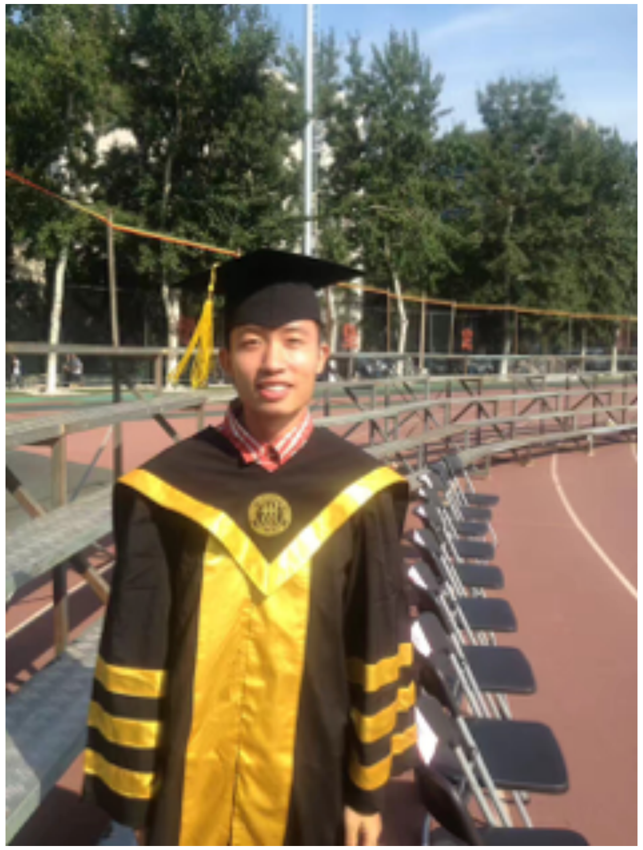

Changle Liu
(Fudan)

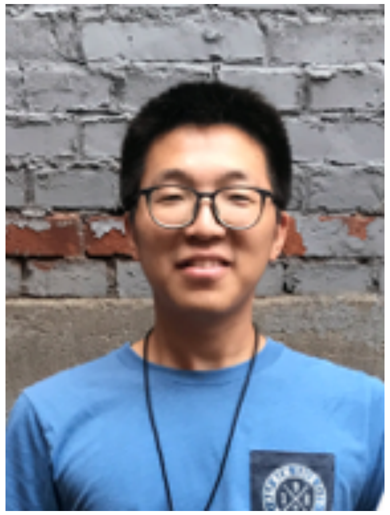

Yao Shen
(Fudan)

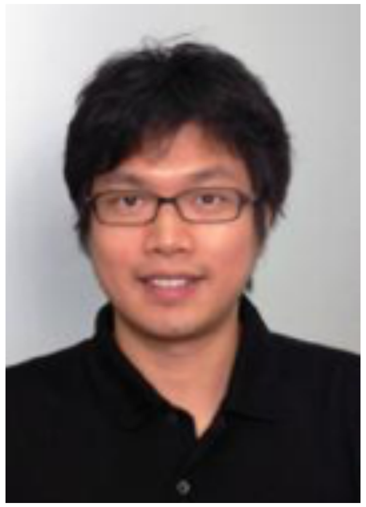

Jun Zhao
(Fudan)

复旦大学
FUDAN UNIVERSITY

approximately thought as non-Kramers doublets

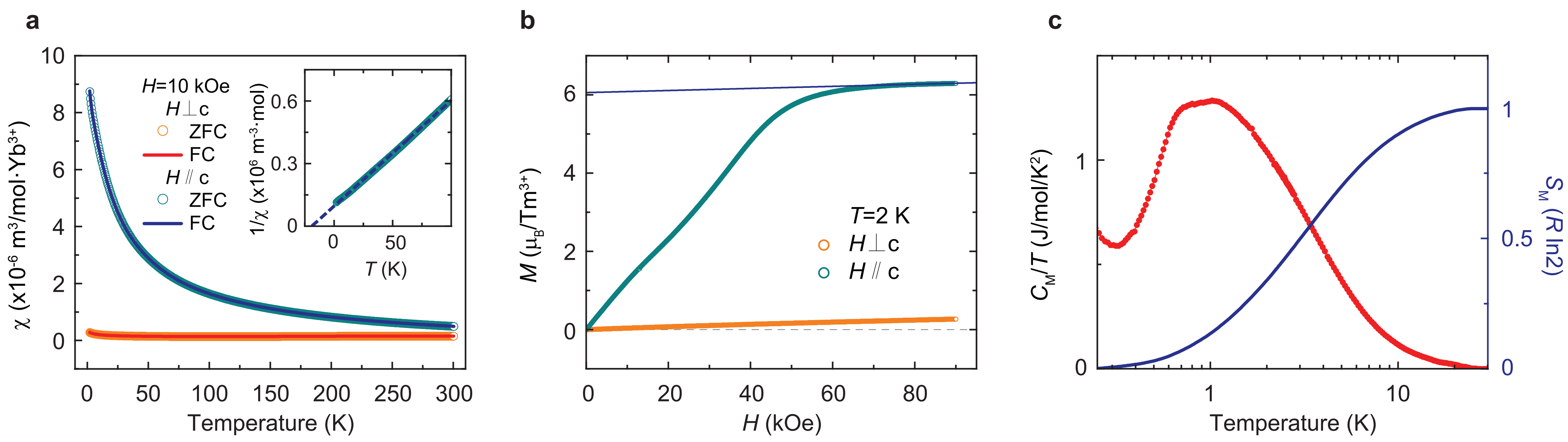

Well-defined spin wave

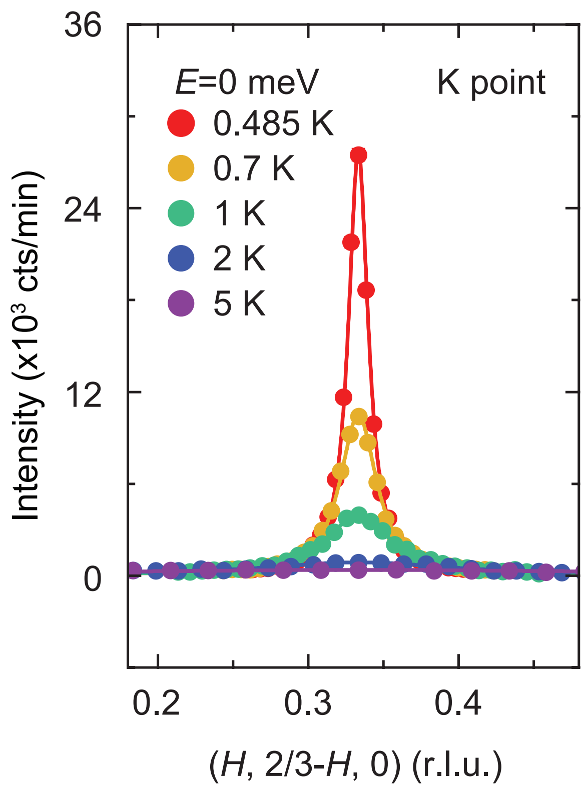

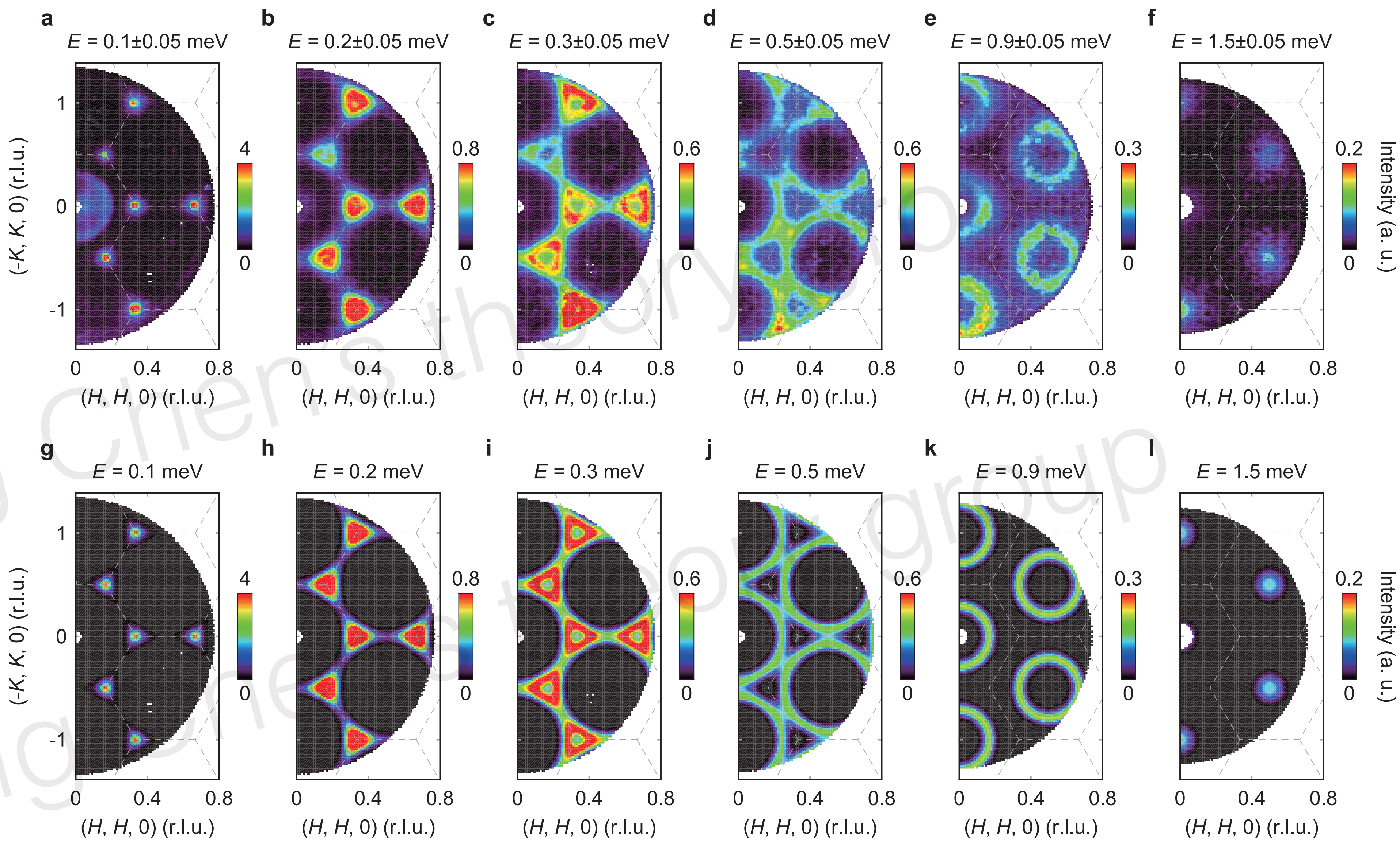

The presence of well-defined spin wave indicates the presence of the hidden order !

Comparison with theory

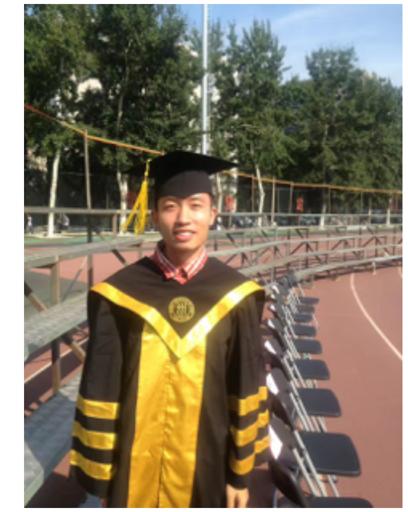

Changle Liu

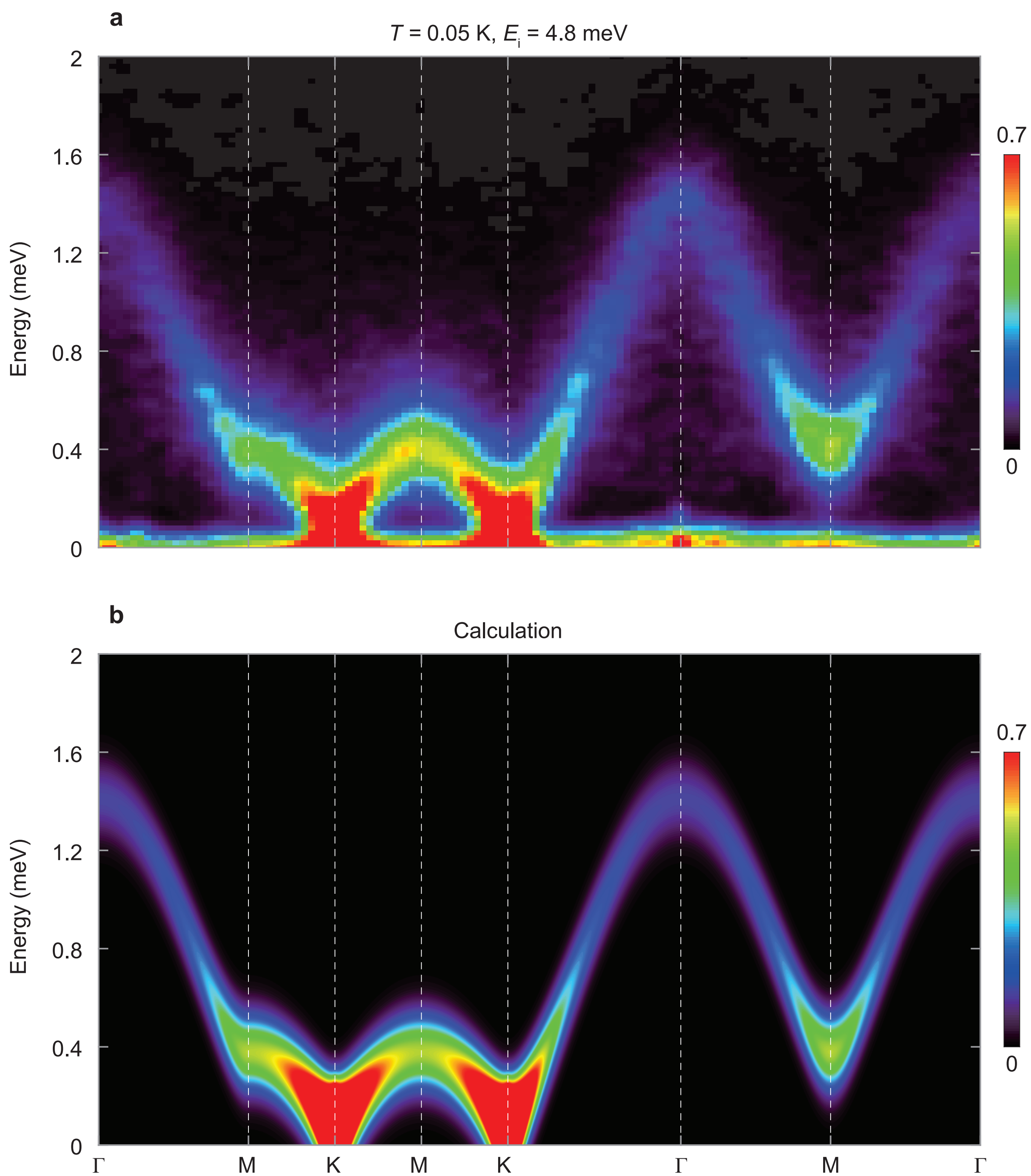

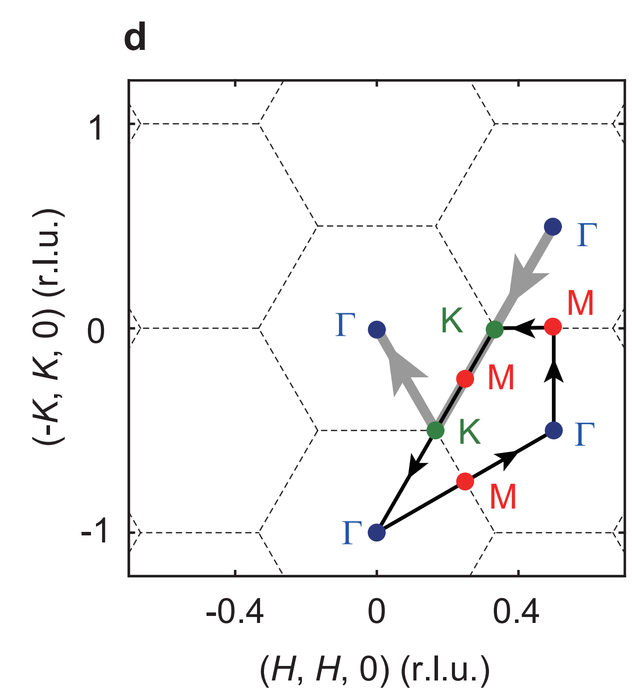

Summary

1. The interplay between geometrical frustration and multipolar local moments leads to rich phases and excitations.

2. The manifestation of the hidden multipolar orders is rather non-trivial, both in the static and dynamic measurements.

3. The non-commutative observables/operators can be used to reveal the dynamics of hidden orders. This is general and can be adapted to many other hidden order systems.

4. Finally, the non-trivial Berry phase effect has not yet been discussed. This thought has been hinted in Kivelson's recent work (PNAS 2018).

復旦大學
FUDAN UNIVERSITY